PUBL. NO. 693
OF THE N.S.M.B.

A METHOD FOR THE CALCULATION OF RESISTANCE AND ~~SAIL~~ SIDE FORCE OF SAILING YACHTS

by Dr Peter van Oossanen, Netherlands Ship Model Basin

Paper presented at the Conference on "Calculator and Computer Aided Design for Small Craft - The Way Ahead" held on March 31/April 1, 1981.

METHOD FOR THE CALCULATION OF THE RESISTANCE AND SIDE FORCE OF SAILING YACHTS

Dr. Peter van Oossanen
Netherlands Ship Model Basin, Wageningen, The Netherlands.

SUMMARY

In this paper a new method for the calculation of the hydrodynamic resistance and side force of sailing craft with an arbitrary hull (canoe body), keel, trim tab, skeg and rudder configuration is presented. The method is based on theoretical resistance and side force formulations, in which the coefficients have been tuned to fit the results of a significant amount of experiments. The results of the method compare satisfactorily with those of full-scale tests on the 5.5 Metre Class Yacht "Antiope". The required calculations can be performed with relative ease on a pocket calculator or (for repeated use) on a small computer.

1. INTRODUCTION

At some stage during the design of a sailing craft the hydrodynamic resistance and side force properties have to be determined for various boat speeds. Usually, a method for the calculation of the resistance and side force of the underwater hull configuration constitutes one of the most important tools of the naval architect-designer. In some cases, speed-related aspects of the hull become dominating factors in the design, often requiring a continuous series of such calculations, culminating in a final check of the design by means of model tests.

This paper presents a new method for the calculation of the resistance and side force of sailing craft with an arbitrary hull (canoe body), keel, trim tab, skeg and rudder configuration. The method is based on mainly theoretical formulations for resistance and side force, of which the (empirical) coefficients have been tuned to fit the results of a significant amount of experiments. The method was developed to predict the resistance and side force performance of 12 Metre Class Yachts for the Americas Cup on which subject a paper was presented by the author in 1979 [1]*. A comparison of the results of this method with those of other calculation procedures and full-scale tests, for the case of the 5.5 Metre Class Yacht "Antiope", was carried out by Larsson [2], who demonstrated that the method adopted to calculate the resistance was exceptionally good. The published comparison for the side force properties of "Antiope" showed that the author's method underestimated the side force by 30 percent. However, an error was made by Larsson in applying the procedure given in Ref. 1. When accounted for, an underestimation of the side force of "Antiope" by 11 percent is obtained instead. Since then, the procedure for the calculation of the side force has been slightly modified (relative to that given in Ref. 1) to take into account the increment in side force on the hull and keel, due to hull-keel interaction, in accordance with results of aerodynamic wing-body studies.

A numerical example of how the method is adopted (for "Antiope") is included in the paper.

* Numbers in brackets refer to the list of references given at the end of the paper.

2. CALCULATION OF THE HYDRODYNAMIC SIDE FORCE

2.1 The Side Force on Keel and Trim Tab

2.1.1 The Basic Equation for the Keel

The side force or lift produced by the keel of a yacht, for small yaw angles β, can be considered to be a linear function of β, analogous to the lift of a wing as a function of angle-of-attack. The basic expression for the side force of a keel can be written as:

$$L_k = \tfrac{1}{2}\rho V_B^2 \frac{\partial C_{L_k}}{\partial \beta} \beta A_k \cos\theta \qquad (1)$$

where L_k = lift (side force) of keel
ρ = density of sea water
V_B = boat speed
β = drift angle
$\frac{\partial C_{L_k}}{\partial \beta}$ = lift-curve slope, i.e. the slope of the lift coefficient curve of the keel (C_{L_k}) against the angle-of-attack (β)
A_k = lateral area of keel
θ = angle of heel of the yacht.

For not too large angles-of-attack, the lift slope of the keel can be considered as a constant for a given keel geometry. The drift angle β is the angle-of-attack at which the hull of the yacht passes through the water. It is measured by the angle between the course and the centre line of the yacht. The angle-of-attack range, or drift-angle range, for which the lift-curve slope is constant, depends primarily on the aspect ratio of the keel. Figure 1, taken from "Fluid-Dynamic Lift" by Hoerner and Borst [3], shows the value of the lift coefficient C_L, as a function of angle-of-attack α, as measured on wings of various aspect ratios AR. The lift coefficient of the keel is defined as:

$$C_{L_k} = \frac{L_k}{\frac{1}{2}\rho V_B^2 A_k \cos\theta} \qquad (2)$$

while the geometric aspect ratio of the keel is defined as:

$$AR_{geom_k} = \frac{b_k}{\bar{c}_k} \qquad (3)$$

where b_k = span (height) of the keel
$\bar{c}_k$ = average chord length of the keel

When the yacht heels at an angle θ, the area of the projection of the keel on a vertical plane is reduced by cos θ, which results in a reduction of the side force.

2.1.2 The Effective Aspect Ratio

It can be shown theoretically that the lift on a wing, protruding from an infinitely long and wide wall, can be derived by neglecting the influence of the wall and by assuming that the effective aspect ratio is doubled through reflection in the wall. In the case of a yacht's keel this also holds since no loss of lift occurs at the keel-hull intersection at moderate angles of heel of the yacht, because the pressure difference between the two sides of the keel is maintained. Hence the effective aspect ratio AR_k can be considered to be double the geometric aspect ratio, viz.:

$$AR_k = \frac{2b_k}{\bar{c}_k} = \frac{2b_k^2}{A_k} \qquad (4)$$

The effect of heel on the effective aspect ratio can be approximately accounted for by reducing the span of the keel by multiplying by cos θ, where θ is the angle of heel, viz.:

$$AR_k = \frac{2b_k^2}{A_k} \cos\theta \qquad (5)$$

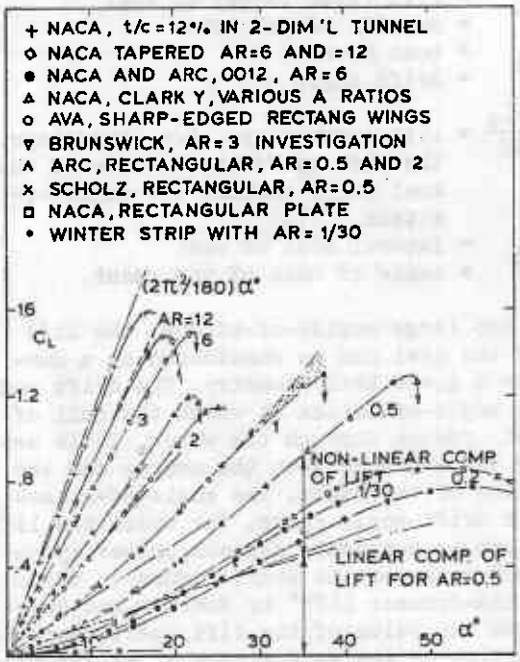

Fig. 1 Lift coefficient of profiled, sharp-edged rectangular (and of some other) wings, as a function of angle of attack (adjusted for zero lift where necessary) for various aspect ratios (from Ref. 3).

2.1.3 The Three-Dimensional Lift-Curve Slope

It follows from Fig. 1 that for one value of the aspect ratio the lift slope is constant, for all practical purposes, up to angles-of-attack varying from about 5 degrees for an aspect ratio of 0.5, to about 10 degrees for an aspect ratio of 1.0, and to about 15 degrees for aspect ratios higher than 6. As the aspect ratio becomes smaller, the non-linear component of lift becomes more important. The non-linear component of lift for an aspect ratio equal to 0.5 becomes discernable at an angle-of-attack of about 5 degrees. Analyses of the performance of sailing yachts have shown that the drift angle β usually attains maximum values of about 7 degrees. In some cases values of up to 10 degrees are found. It follows that in the present context the assumption of a constant lift slope value is valid for values of the (effective) aspect ratio in excess of about 1.0, or for geometric aspect ratio values in excess of about 0.5. For smaller aspect ratios the concept of a constant lift-curve slope could lead to an underestimation of the side force of the keel.

Various formulations have been derived which express the value of the 3-dimensional lift-curve slope as a function of the (effective) aspect ratio. A widely-used formulation is that derived by Whicker and Fehlner [4]. The relation obtained by them is valid for the lift-curve slope, at zero angle-of-attack, of control surfaces (rudders, keels, etc.) with a taper ratio λ equal to 0.45*. This value of the taper ratio nearly leads to elliptical spanwise loading for a quarter-chord, sweep-angle of zero. Also, the Whicker and Fehlner relation is valid for square tip shapes. For rounded planforms and rounded lateral edges the lift-curve slope is markedly reduced, particularly at low aspect ratios while, according to Hoerner and Borst [3], the lift-curve slope for differing taper ratios is hardly affected. To account for the effect of rounded planforms and rounded lateral edges on the lift-curve slope, the concept of an "effective span" can be adopted. This concept leads to the possibility of deriving the lift-curve slope of keels and rudders with rounded planforms or rounded lateral edges (or both) from the Whicker and Fehlner lift-curve slope equation, valid for tapered control surfaces with square tips. The Whicker and Fehlner relation, in the present nomenclature, is as follows:

$$\left(\frac{\partial C_{L_k}}{\partial \beta}\right)_{square} = \frac{2\pi a_{o_k} AR_k}{2a_{o_k} + \cos\Lambda_k \sqrt{AR_k^2/\cos^4\Lambda_k + 4}} \qquad (6)$$

where a_{o_k} = lift-curve slope factor of the 2-dimensional section shape composing the keel (a value equal to 1.0 corresponds to the theoretical lift-curve slope of 2π),
Λ_k = sweep-angle of quarter-chord line of keel.

*The taper ratio λ is defined as the ratio of the chord length at the tip to that at the root of the rudder or keel.

TABLE I Typical values for the effective span ratio $\Delta b/b$

planform	lateral edges	$\Delta b/b$	$(1+\Delta b/b)^2$
- Rectangular or tapered	sharp	0	1.0
- Elliptical or rounded	sharp	-0.04	0.92
- Rectangular or tapered	round	-0.09	0.83
- Rounded	round	-0.12	0.78
- Delta type	round	-0.12	0.78

For round planforms and for round lateral edges:

$$\left(\frac{\partial C_{L_k}}{\partial \beta}\right)_{round} = (1+\Delta b/b)^2 \left(\frac{\partial C_{L_k}}{\partial \beta}\right)_{square} \qquad (7)$$

Where Δb is the effective reduction of the geometric span b. Hoerner and Borst [3] list values for $\Delta b/b$, which are presented here in Table I.

The marked reduction in $\Delta b/b$ for rounded planforms and rounded lateral edges listed in Table I is due to the inward movement of the trailing (or free) vortices near the tip, leading to a reduction in the "vortex span" (see e.g. Fig. 10, page 3-7 of Hoerner and Borst [3]).

The symbols used here and elsewhere in this paper, relative to the keel of a yacht, are defined in Fig. 2.

2.1.4 The Two-Dimensional Lift-Curve Slope

For individual design calculations, after the section profile to be used for the keel has been selected, it is appropriate to determine the 2-dimensional lift-curve slope from the results of tests, as tabulated e.g. by Riegels [5] and Abbott and Doenhoff [6]. For parametric design studies, however, it is often more practical to use a relation between a_o and the parameters on which it is dependent. Besides the thickness-chord ratio, Hoerner and Borst [3] conclude that the trailing-edge "wedge" angle of the section shape is also important. Sections with cusped contours near the trailing edge (leading to small trailing-edge angles) such as the NACA 63 and 64 series, have high lift-curve slopes. Sections such as the NACA 4-digit series, with relative large trailing-edge angles, display a significantly lower lift-curve slope. On the basis of these facts the following relation was obtained for the 2-dimensional lift-curve slope factor a_{o_k}:

$$a_{o_k} = \frac{\left(\frac{dC_L}{d\alpha}\right)_{\alpha=0}}{2\pi} = 1+0.82\,(t/c)_k - \tan\tau_{T_k}\left(\frac{0.117}{(t/c)_k} + 3.2(t/c)_k + 3.9(t/c)_k^2\right) \qquad (8)$$

where:

$\left(\frac{dC_L}{d\alpha}\right)_{\alpha=0}$ = 2-dimensional lift-curve slope at zero angle-of-attack

$(t/c)_k$ = thickness-chord ratio of section shape of keel

τ_{T_k} = half trailing-edge angle of section shape of keel.

Figure 3 shows how the angle τ_{T_k} and the ratio $(t/c)_k$ are defined. Sometimes the angle τ_{T_k} is not given. In that case the value of τ_{T_k} can be found from the slope at the trailing edge (ε_{T_k}) by use of the following relation:

$$\tan\tau_{T_k} = \varepsilon_{T_k} \cdot (t/c)_k \qquad (9)$$

Riegels [5] has listed values for ε_{T_k} for most known section shapes.

Comparisons between the values following from equation 8 and experimental values for the NACA 00, 23, 63, 64, 65, 66 and some DVL profiles are given in Fig. 4. The a_o values for the NACA 63, 64, 65 and 66 profiles were taken from Abbott and Doenhoff [6], who (in Fig. 57) give a set of figures showing $dC_L/d\alpha$ (α in degrees) as a function of thickness-chord ratio for a Reynolds number of 6×10^6. They provide a faired curve for each type of section, for both smooth and rough surface conditions. The experimental values for the NACA 00 and 23 series were taken from Riegels [5] for a Reynolds number of 8.2×10^6 to 8.4×10^6. At a Reynolds number of 6×10^6, the lift-curve slopes of these sections are locally about 5 to 10 percent higher. The experimental values for the DVL profiles were also taken from Riegels, and are valid for Reynolds numbers varying between 2.5×10^6 to 3.2×10^6.

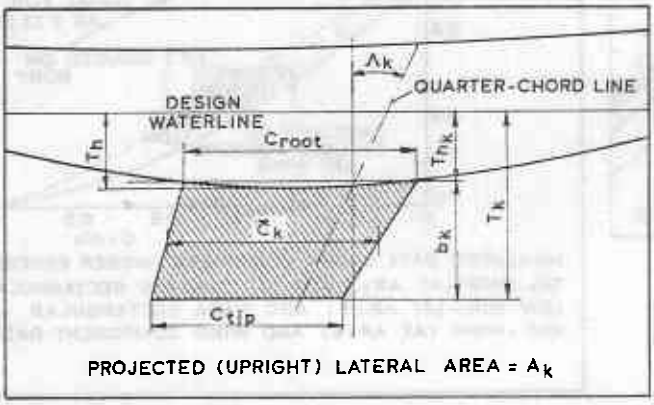

Fig. 2 Definition of symbols used to describe the geometry of a keel.

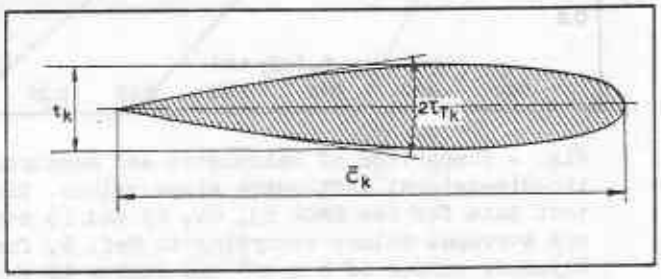

Fig. 3 Definition of symbols used to describe the average (mean) section of a keel.

As follows from Fig. 4, the calculated and experimental values for a_o agree satisfactorily for all practical purposes. Equation 7 can be used for most types of sections for Reynolds numbers in excess of 2×10^6 and for camber-chord ratios up to about 0.04.

2.1.5 The Effect of Hull-Keel Interaction on the Hydrodynamic Side Force

The presence of the hull influences the flow along the keel and the presence of the keel changes the flow along the hull. As described by Schlichting and Truckenbrodt [7], additional velocities are induced along the hull by the keel which are directed to windward in front of the keel and to leeward behind the keel. The hull is therefore in a curved flow which influences (increases) the side force on the hull. The effect of this cross flow along the hull on the flow about the keel is to induce additive upwash velocities in the vicinity of the keel which effectively increases the angle-of-attack to about 2α just where the keel intersects the hull. It follows that the presence of the hull increases the side force on the keel. Both effects will be accounted for in this section because the adopted method uses the basic lift of the keel, as follows from equation 1, to calculate the increment in side force on the hull and on the keel.

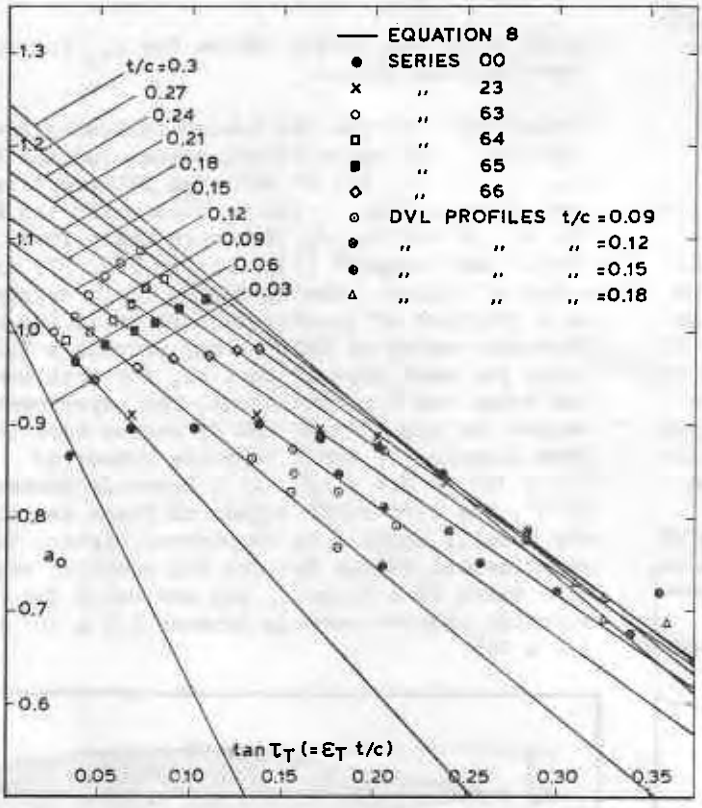

Fig. 4 Comparison of calculated and measured two-dimensional lift-curve slope values. The test data for the NACA 63, 64, 65 and 66 series are averaged values according to Ref. 6, for a Reynolds number of 6×10^6 and camber to chord ratios of up to 0.04. The test data for the NACA 00 (4 digit) and 23 series, and for the DVL sections, are those given in Ref. 5, for Reynolds number values ranging from 2.5×10^6 to 8.5×10^6.

In aerodynamics, the effect of interactions between a wing and the fuselage of an airplane, on the total lift, poses a similar problem to that of the keel and the hull of a sailing craft. In a review on this topic, Ashley and Rodden [8] conclude that the net effect of centering an elongated fuselage of circular cross-section in a wing is to slightly increase the total lift of fuselage (hull) and wing (keel) over that of the wing alone, for small ratios of fuselage diameter to wingspan. For large fuselage diameter to wingspan ratios the total lift decreases with respect to that of the wing alone. This can be seen in Fig. 5, taken from Hoerner and Borst [3], in which the increments in the lift-curve slope of wing-fuselage combinations due to interaction effects, for effective aspect ratios greater than 3, are shown as a function of the fuselage diameter-wingspan ratio, $\sigma = d/b$. From this figure it follows that the total side force produced by keel and hull, for hull draught - keel depth ratios up to about 0.4 or 0.5 can be calculated with reasonable accuracy by assuming that the keel extends to the waterline and setting the total hull-keel lift equal to the side force of this "equivalent" keel for which $\sigma = 0$. Indeed, this procedure was first suggested by Gerritsma [9], and has been used with success by Beukelman and Keuning [10], and others. One drawback of this "equivalent" keel method, however, is that it does not provide any insight into the relative significance of the side force of the hull itself or the side force increments on hull and keel due to interaction effects. Also, for hull draught to keel depth ratios in excess of about 0.5 and for geometric aspect ra-

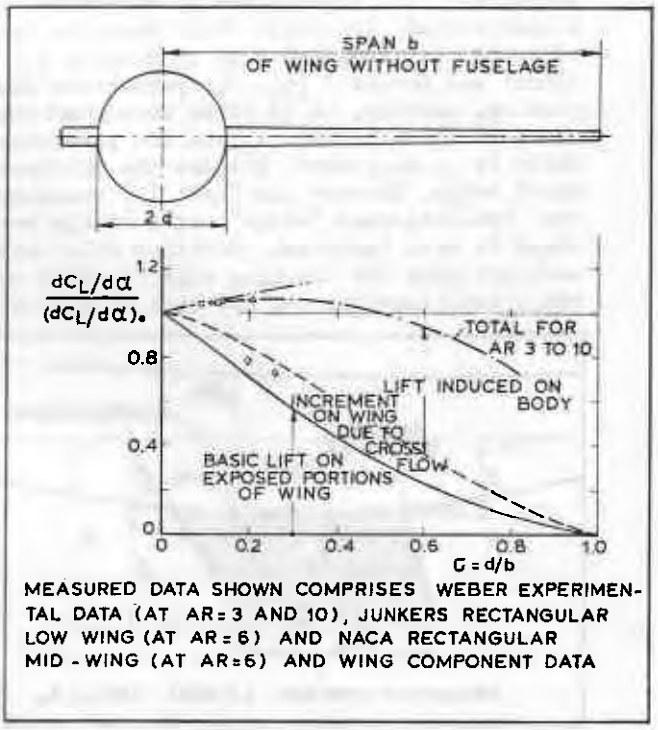

Fig. 5 The lift-curve slope of wing-fuselage combinations as a function of the diameter ratio d/b (from Ref. 3).

tios smaller than about 1.5, the "equivalent" keel method will overestimate the side force. For these reasons the results derived by Flax [11] are here preferred, who derived approximate formulae for the separate interaction effects mentioned above, approximately valid for small to moderate aspect ratios, typical of yacht keels. When applied to the hull-keel case under consideration, these formulae are as follows:

$$\Delta L_k = \sigma L_k \qquad (10)$$

$$\Delta L_h = \sigma(1+\sigma)L_k \qquad (11)$$

where:

ΔL_k = side force increment induced on keel due to cross flow on hull

ΔL_h = side force increment induced on hull by the keel

L_k = side force of exposed part of keel alone (without keel-hull interaction) as follows from equation 1

σ = hull draught to keel depth ratio ($=T_{h_k}/T_k$; see Fig. 2).

The total side force produced by the keel, comprising the total lift on the keel and the lift induced on the hull by the keel, then becomes:

$$L_{T_k} = L_k + \Delta L_k + \Delta L_h = (1+\sigma)^2 L_k \quad \text{or} \qquad (12)$$

$$L_{T_k} = \tfrac{1}{2}\rho V_B^2 \frac{\partial C_{L_k}}{\partial \beta} \cdot \beta \cdot \left(1+\frac{T_{h_k}}{T_k}\right)^2 A_k \cos\theta \qquad (13)$$

Figure 6 shows a comparison between the results of Vladen [12], valid for geometric aspect ratios greater than about 1.5, the results of Flax [11] as used in equations 10 and 11, and slender wing theory as presented by Schlichting and Truckenbrodt [7], for the ratio of the lift of a wing alone (without body influence) to the sum of the lift of the wing-body configuration.

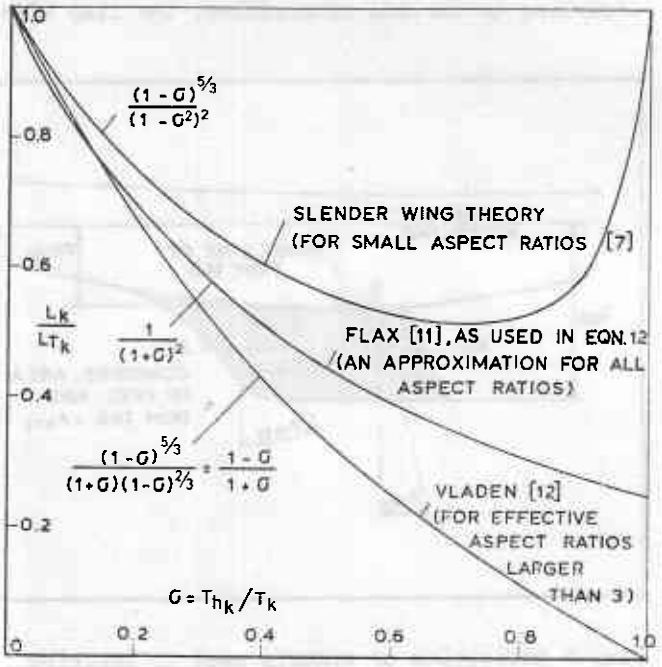

Fig. 6 Ratio of side force on the keel alone (without interaction) to the sum of the total side force on the keel (with interaction) and the keel-induced side force on the hull according to 3 different approximations.

2.1.6 The Effect of a Trim Tab on the Side Force of the Keel

2.1.6.1 The Basic Equation

The effect of a trim tab on the side force of the keel is analogous to the effect of a moveable flap in a wing of an airplane. A flap deflection downward causes an increase in the effective camber of the wing and hence an increase in lift. The curves of lift coefficient against angle-of-attack, for several flap deflection angles, are therefore parallel to each other.

If the angle of deflection of the trim tab is δ_{tt}, the dependence of the side force of a keel on the drift angle β and the trim tab angle can be written as:

$$C_{L_{ktt}} = \frac{\partial C_{L_{ktt}}}{\partial \beta}\beta + \frac{\partial C_{L_{ktt}}}{\partial \delta_{tt}}\delta_{tt} \quad \text{or} \qquad (14)$$

$$C_{L_{ktt}} = \frac{\partial C_{L_{ktt}}}{\partial \beta}\left(\beta + \frac{\partial \beta}{\partial \delta_{tt}}\delta_{tt}\right) \qquad (15)$$

where the subscript ktt implies that the respective value of the combined keel and trim tab configuration is to be adopted. The total side force of a keel-trim tab configuration then becomes (see equation 13):

$$L_{T_{ktt}} = \tfrac{1}{2}\rho V_B^2 \frac{\partial C_{L_{ktt}}}{\partial \beta}\left(\beta + \frac{\partial \beta}{\partial \delta_{tt}}\delta_{tt}\right)\left(1+\frac{T_{h_{ktt}}}{T_{ktt}}\right)^2 A_{ktt}\cos\theta \qquad (16)$$

The linear relations 14 and 15 are approximately valid for trim tab angles from -10 to +10 degrees. The coefficient $\partial\beta/\partial\delta_{tt}$ is commonly referred to as the flap effectiveness ratio. Figure 7 shows a typical result of the effect of a flap on the lift of a wing, while Fig. 8 shows the dependency of the flap effectiveness ratio on the

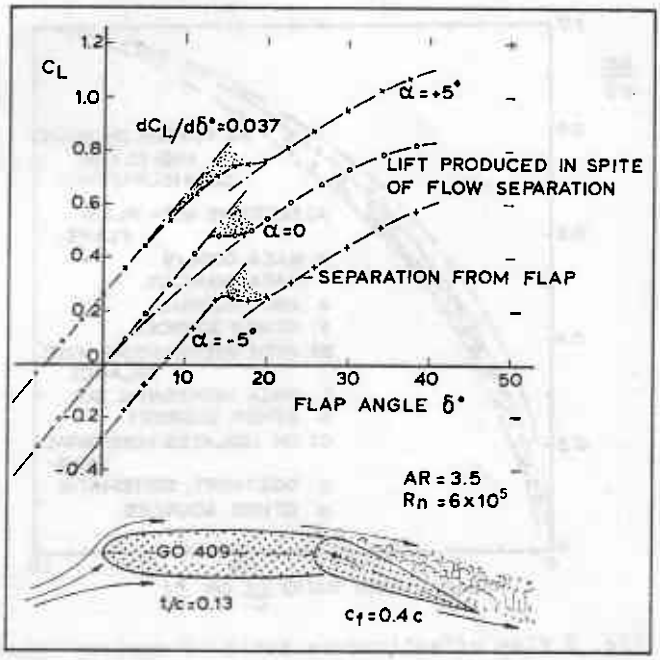

Fig. 7 Lifting characteristics of an isolated rectangular horizontal tail surface with flap tested in an open wind tunnel (from Ref. 3).

flap-wing chord ratio. Both figures are taken from Hoerner and Borst [3]. When the chord length of the trim tab is not constant over the height of the keel, as is sometimes the case, it is more appropriate to use the ratio of the trim tab area to the (total) keel area A_{tt}/A_{ktt}, instead of the ratio of the trim tab chord to the (total) chord C_{tt}/C_{ktt}. A typical trim tab configuration is shown in Fig. 9.

2.1.6.2 The Flap Effectiveness Ratio

For a flapped wing (keel) of infinite aspect ratio and small flap (trim tab) angles, Glauert [13] derived a theoretical expression for the flap effectiveness ratio $\partial\beta/\partial\delta_{tt}$. The derived expression (valid for zero wing and zero flap thickness), in terms of the keel-trim tab nomenclature is:

$$\left(\frac{\partial\beta}{\partial\delta_{tt}}\right)_{th} = \frac{2}{\pi}\left(\sqrt{A_{tt}/A_{ktt}\,(1-A_{tt}/A_{ktt})} + \right.$$

$$\left. + \arcsin\sqrt{A_{tt}/A_{ktt}}\right) \qquad (17)$$

The curve denoted as "theory" in Fig. 8 is that according to equation 17. From Fig. 8 it follows that due to viscous effects, experimental values for the flap effectiveness ratio are always smaller than the theoretical values. Since the differences can be of the order of 10 to 20 percent or more for frequently used section shapes and values of A_{tt}/A_{ktt}, it is appropriate to correct equation 17 to yield more realistic values. The observation that the effectiveness ratio is reduced by section thickness and particularly by the trailing-edge "wedge" angle $\tau_{T_{tt}}$ (see Hoerner and Borst [3], page 9-3) led, through application of a trial and error procedure, to the following equation for the flap effectiveness ratio, corrected for the effects of viscosity:

$$\left(\frac{\partial\beta}{\partial\delta_{tt}}\right)_o = \left(\frac{\partial\beta}{\partial\delta_{tt}}\right)_{th}\left(0.75+0.25\left(\frac{A_{tt}}{A_{ktt}}\right)^{0.1} + \right.$$

$$\left. - 7.35\left(1-\left(\frac{A_{tt}}{A_{ktt}}\right)^{0.1}\right)\tan\tau_{T_{tt}}\right) \qquad (18)$$

In equation 18, $\tau_{T_{tt}}$ is half the trailing-edge "wedge" angle of the trim tab (see also equation 8). Values for the effectiveness ratio according to equation 18 are shown in Fig. 10 together with some measured values. Values for the ratio of the corrected to the theoretical flap effectiveness value is given as a function of $\tan\tau_{T_{tt}}$, for various trim tab-keel area ratios.

2.1.6.3 Effects of Finite Aspect Ratio and Sweep Angle

According to Hoerner and Borst [3], the flap effectiveness ratio only slightly varies down to aspect ratios equal to about 2. For smaller aspect ratios, experimental and lifting surface theory results indicate that as the aspect ratio decreases, the flap effectiveness increases. The flap effectiveness approaches unity as the aspect ratio approaches zero.

From results compiled by Hoerner and Borst [3], shown in Fig. 11, it is apparent that the effect of aspect ratio is noticeable for flap effectiveness values, as calculated from equation 18, larger than about $0.17\ AR_{ktt}$, where AR_{ktt} is the effective aspect ratio of the keel-trim tab configuration, as follows from equation 5. An approximation of this influence of the aspect ratio was found by assuming that when $\partial\beta/\partial\delta_{tt} > 0.17\ AR_{ktt}$, the effectiveness tends to unity as does a $1-(\sin x)^{0.25}$ function. The actual equation obtained is:

$$\frac{\partial\beta}{\partial\delta_{tt}} = 1-\left(1-\left(\frac{\partial\beta}{\partial\delta_{tt}}\right)_o\right)\left(\sin\frac{0.17\pi AR_{ktt}}{2\left(\partial\beta/\partial\delta_{tt}\right)_o}\right)^{0.25} \qquad (19)$$

$$\text{when } \left(\frac{\partial\beta}{\partial\delta_{tt}}\right)_o > 0.17\ AR_{ktt}$$

According to various authorities, the flap effec-

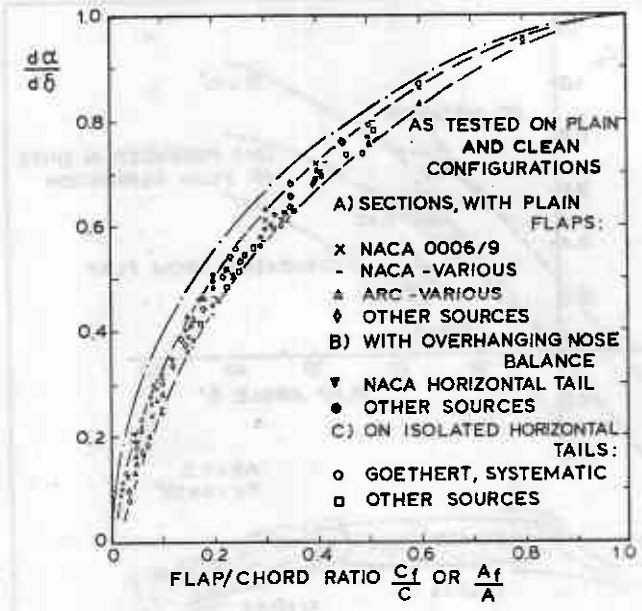

Fig. 8 Flap effectiveness ratio of various types of trailing-edge control flaps (elevators, rudders, ailerons) as a function of their chord ratio (from Ref. 3).

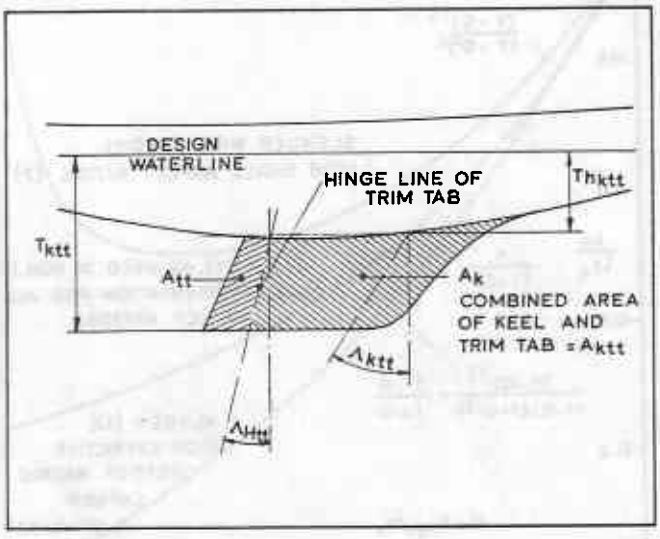

Fig. 9 Definition of symbols used to describe the geometry of a keel and trim tab configuration.

tiveness ratio varies with the cosine of the sweepback angle of the hinge line of the flap $\Lambda_{H_{tt}}$ [3]. Hence equation 18 should be multiplied by $\cos \Lambda_{H_{tt}}$ when the hinge line of the trim tab has sweepback, as follows:

$$\left(\frac{\partial\beta}{\partial\delta_{tt}}\right)_o = \left(\frac{\partial\beta}{\partial\delta_{tt}}\right)_{th}\left(0.75+0.25\left(\frac{A_{tt}}{A_{ktt}}\right)^{0.1} + \right.$$
$$\left. - 7.35\left(1-\left(\frac{A_{tt}}{A_{ktt}}\right)^{0.1}\right)\tan\tau_{T_{tt}}\right)\cos\Lambda_{H_{tt}} \qquad (20)$$

2.1.7 The Final Equations for the Side Force of Keel and Trim Tab

On the basis of the results presented on the preceding pages, the total side force of a keel-trim tab configuration, including the side force on the hull induced by the keel, can be calculated as follows:

$$L_{T_{ktt}} = \tfrac{1}{2}\rho V_B^2 \frac{\partial C_{L_{ktt}}}{\partial\beta}\left(\beta + \frac{\partial\beta}{\partial\delta_{tt}}\delta_{tt}\right)\left(1+\frac{T_{h_{ktt}}}{T_{ktt}}\right)^2 A_{ktt}\cos\theta \qquad (16)$$

where:

$$\frac{\partial C_{L_{ktt}}}{\partial\beta} = \frac{2\pi a_{o_{ktt}}\left(1+\Delta b/b\right)^2}{2a_{o_{ktt}} + \cos\Lambda_{ktt}\sqrt{AR_{ktt}^2/\cos^4\Lambda_{ktt}+4}} \qquad (6)+(7)$$

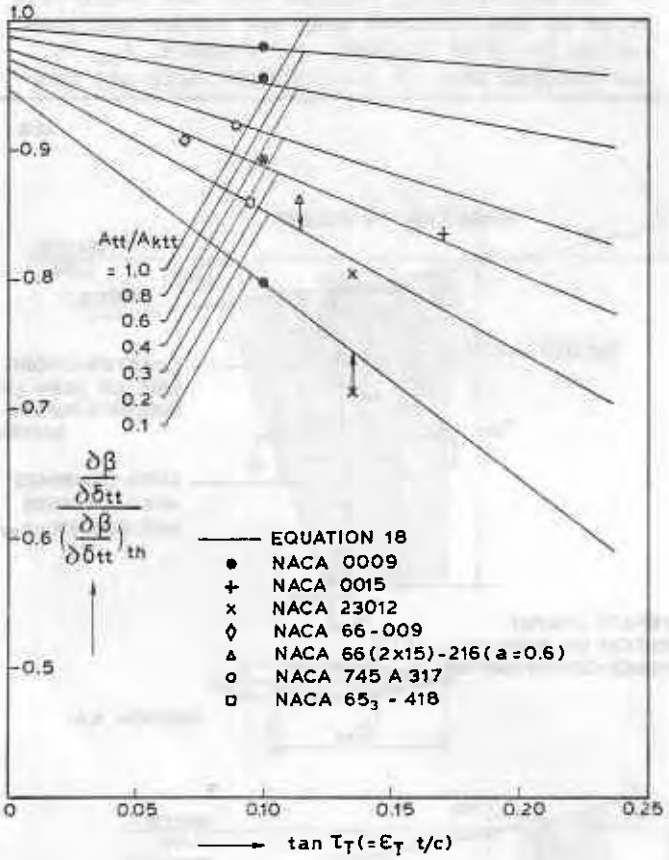

Fig. 10 Comparison of calculated and measured flap effectiveness ratio values. The test data shown are from Refs. 3 and 6, for Reynolds number values ranging from 1.4×10^6 to 8×10^6, for plain flaps with sealed gaps. Only the infinite aspect ratio case is considered.

in which:

$$a_{o_{ktt}} = 1+0.82(t/c)_{ktt} - \tan\tau_{T_{tt}}\left(\frac{0.117}{(t/c)_{ktt}} + \right.$$
$$\left. + 3.2(t/c)_{ktt} + 3.9(t/c)_{ktt}^2\right) \qquad (8)$$

and

$$\frac{\partial\beta}{\partial\delta_{tt}} = 1-\left(1-\left(\frac{\partial\beta}{\partial\delta_{tt}}\right)_o\right)\left(\sin\frac{0.17\pi AR_{ktt}}{2\left(\partial\beta/\partial\delta_{tt}\right)_o}\right)^{0.25} \qquad (19)$$

in which

$$\left(\frac{\partial\beta}{\partial\delta_{tt}}\right)_o = \left(\frac{\partial\beta}{\partial\delta_{tt}}\right)_{th}\left(0.75+0.25\left(\frac{A_{tt}}{A_{ktt}}\right)^{0.1} + \right.$$
$$\left. - 7.35\left(1-\left(\frac{A_{tt}}{A_{ktt}}\right)^{0.1}\right)\tan\tau_{T_{tt}}\right)\cos\Lambda_{H_{tt}} \qquad (20)$$

where

$$\left(\frac{\partial\beta}{\partial\delta_{tt}}\right)_{th} = \frac{2}{\pi}\left(\sqrt{A_{tt}/A_{ktt}\left(1-A_{tt}/A_{ktt}\right)} + \right.$$
$$\left. + \arcsin\sqrt{A_{tt}/A_{ktt}}\right) \qquad (17)$$

It should be noted that when $\left(\partial\beta/\partial\delta_{tt}\right)_o < 0.17AR_{ktt}$, then $\partial\beta/\partial\delta_{tt} = \left(\partial\beta/\partial\delta_{tt}\right)_o$. The effective aspect ratio of the keel-trim tab configuration is:

$$AR_{ktt} = \frac{2b_{ktt}}{\bar{c}_{ktt}}\cos\theta = \frac{2b_{ktt}^2}{A_{ktt}}\cos\theta = \frac{2\left(T_{ktt}-T_{h_{ktt}}\right)^2\cos\theta}{A_{ktt}} \qquad (5)$$

When a trim tab is not fitted to the keel, or when $\delta_{tt}=0$, the total side force of the keel becomes:

$$L_{T_k} = \tfrac{1}{2}\rho V_B^2 \frac{\partial C_{L_k}}{\partial\beta}\beta\left(1+\frac{T_{h_k}}{T_k}\right)^2 A_k\cos\theta \qquad (13)$$

with

$$\frac{\partial C_{L_k}}{\partial\beta} = \frac{2\pi a_o AR_k\left(1+\Delta b/b\right)^2}{2a_o+\cos\Lambda_k\sqrt{AR_k^2/\cos^4\Lambda_k+4}} \qquad (6)+(7)$$

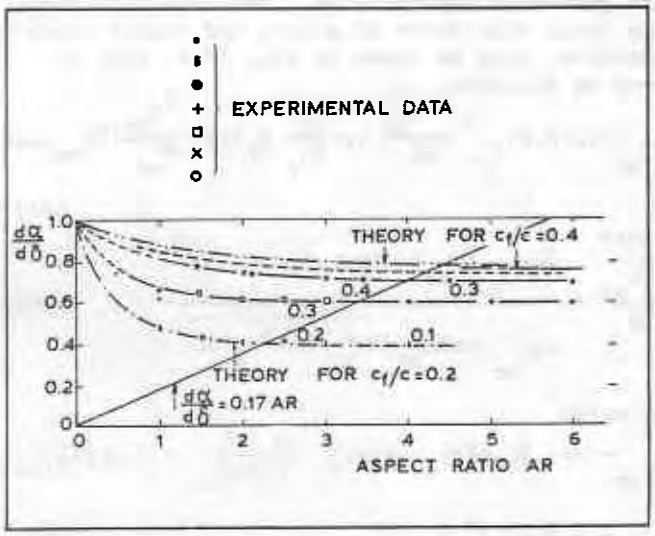

Fig. 11 Influence of the aspect ratio upon the flap effectiveness ratio (from Ref. 3).

where

$$a_o = 1+0.82(t/c)_k-\tan\tau_k\left(\frac{0.117}{(t/c)_k} + 3.2(t/c)_k + 3.9\,(t/c)_k^2\right) \quad (8)$$

where

$$AR_k = \frac{2(T_k-T_{h_k})^2\cos\theta}{A_k} \quad (5)$$

2.2 The Side Force on Skeg and Rudder

2.2.1 Side Force on a Combined Skeg and Rudder Configuration

The total side force on a combined skeg and rudder configuration, such as depicted in Fig. 12a, can be determined along the same lines as presented in section 2.1 for a keel-trim tab configuration when the entities related to the skeg and those related to the rudder take the place of those of the keel and the trim tab, respectively. Two additional corrections to the formulas must be made, however. The first of these corrections is for the speed of the flow relative to the rudder. Since the rudder is located in the wake (downwash) of the keel, it is appropriate to assume that its effective speed through the water is not equal to V_B. Also, the thickness of the boundary layer along the hull at the location of the rudder is relatively greater than at the location of the keel. To correct for these effects, it is assumed that the effective speed of the rudder through the water is equal to approximately $0.8V_B$. Secondly, the rudder is often situated close to the transom or stern of the yacht, in which case the hull-rudder intersection is often above the water surface. In this case the effective aspect ratio is no longer double the geometric aspect ratio, but appreciably less. It is assumed that then the effective aspect ratio approximately equals the geometric aspect ratio. The equations for the total side force of a skeg and rudder configuration, such as shown in Fig. 12 a, then become as follows:

$$L_{T_{sr}} = \tfrac{1}{2}\rho(0.8V_B)^2 \frac{\partial C_{L_{sr}}}{\partial\beta}\left(\beta+\frac{\partial\beta}{\partial\delta_r}\delta_r\right)\left(1+\frac{T_{h_{sr}}}{T_{sr}}\right)^2 A_{sr}\cos\theta \quad (21)$$

where

$$\frac{\partial C_{L_{sr}}}{\partial\beta} = \frac{2\pi a_{o_{sr}} AR_{sr}(1+\Delta b/b)^2}{2a_{o_{sr}} + \cos\Lambda_{sr}\sqrt{AR_{sr}^2/\cos^4\Lambda_{sr}+4}} \quad (22)$$

in which

$$a_{o_{sr}} = 1+0.82(t/c)_{sr}-\tan\tau_{T_r}\left(\frac{0.117}{(t/c)_{sr}} + 3.2(t/c)_{sr} + 3.9(t/c)_{sr}^2\right) \quad (23)$$

and

$$\frac{\partial\beta}{\partial\delta_r} = 1-\left(1-\left(\frac{\partial\beta}{\partial\delta_r}\right)_o\right)\left(\sin\frac{0.17\pi AR_{sr}}{2(\partial\beta/\partial\delta_r)_o}\right)^{0.25} \quad (24)$$

where

$$\left(\frac{\partial\beta}{\partial\delta_r}\right)_o = \left(\frac{\partial\beta}{\partial\delta_r}\right)_{th}\left(0.75+0.25(A_r/A_{sr})^{0.1}-7.35\left(1-(A_r/A_{sr})^{0.1}\right).\tan\tau_{T_r}\right)\cos\Lambda_{H_r} \quad (25)$$

and

$$\left(\frac{\partial\beta}{\partial\delta_r}\right)_{th} = \frac{2}{\pi}\left(\sqrt{A_r/A_{sr}(1-A_r/A_{sr})} + \arcsin\sqrt{A_r/A_{sr}}\right) \quad (26)$$

Again, when $(\partial\beta/\partial\delta_r)_o < 0.17\,AR_{sr}$, then $\partial\beta/\partial\delta_r=(\partial\beta/\partial\delta_r)_o$.

The effective aspect ratio follows from the following relations:

$$AR_{sr} = \frac{2(T_{sr}-T_{h_{sr}})^2\cos\theta}{A_{sr}} \quad \text{for } T_{h_{sr}} > 0 \quad (27)$$

and

$$AR_{sr} = \frac{T_{sr}\cos\theta}{\bar{c}_{sr}} \quad \text{for } T_{h_{sr}} \le 0 \quad (28)$$

The case of $T_{h_{sr}} \le 0$ occurs when the hull-rudder intersection is above the water surface. Then the value of $(1+T_{h_{sr}}/T_{sr})^2$ in equation 21 becomes equal to unity. In equation 21 through 28 the subscript sr implies that the respective value of the combined skeg and rudder configuration is to be adopted. For example, A_{sr} is the lateral area of the combined skeg and rud-

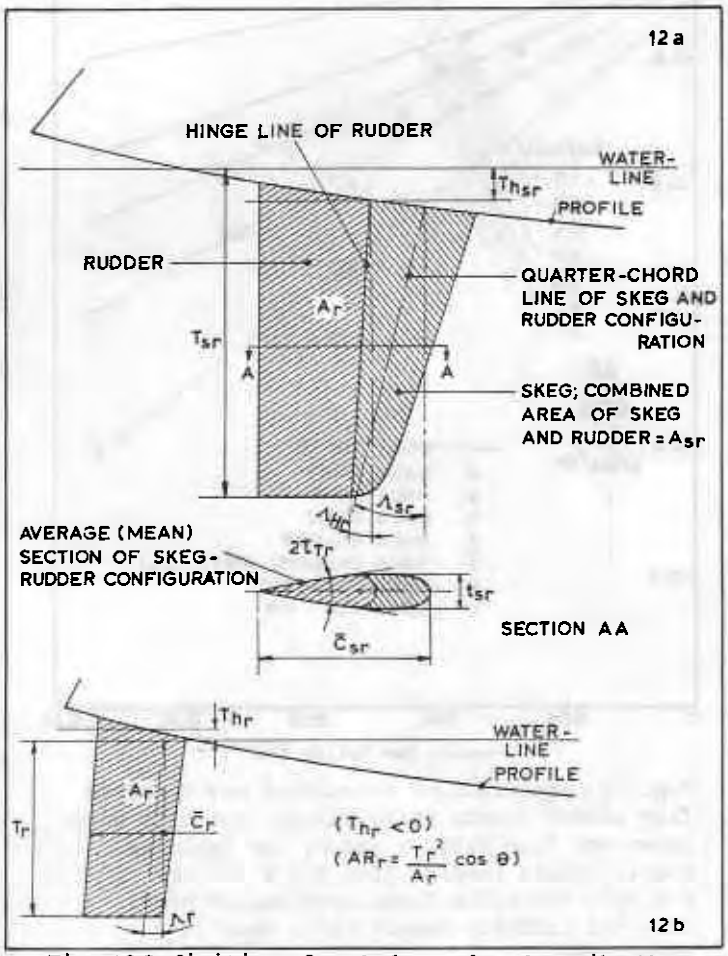

Fig. 12 Definition of symbols used to describe the geometry of a skeg and rudder configuration (Fig. 12a), and of a rudder-alone (Fig. 12b), for which the case $T_{hr}<0$ is drawn.

der configuration. Similarly, the subscript r implies that the respective value of the rudder is to be taken only. For example δ_r is the rudder angle and τ_{T_r} is the half trailing-edge angle of the rudder section. The quantities used in these equations are defined in Fig. 12a.

2.2.2 Side Force on a Rudder Alone

The side force on a spade-type rudder, as depicted in Fig. 12b, at zero rudder angle, can be determined from an equation similar to equation 13 valid for a keel without a trim tab. In general, the side force on a rudder at any angle δ_r becomes as follows:

$$L_{T_r} = \tfrac{1}{2}\rho(0.8V_B)^2 \frac{\partial C_{L_r}}{\partial \beta}(\beta+\delta_r)\left(1+\frac{T_{h_r}}{T_r}\right)^2 A_r \cos\theta \qquad (29)$$

where, as before:

$$\frac{\partial C_{L_r}}{\partial \beta} = \frac{2\pi a_{o_r} AR_r (1+\Delta b/b)^2}{2a_{o_r}+\cos\Lambda_r \sqrt{AR_r^2/\cos^4\Lambda_r+4}} \qquad (30)$$

in which

$$a_{o_r} = 1+0.82(t/c)_r - \tan\tau_{T_r}\left(\frac{0.117}{(t/c)_r}+3.2(t/c)_r + 3.9(t/c)_r^2\right) \qquad (31)$$

where

$$AR_r = \frac{2(T_r-T_{h_r})^2\cos\theta}{A_r} \quad \text{when } T_{h_r} > 0 \qquad (32)$$

and

$$AR_r = \frac{T_r\cos\theta}{c_r} \quad \text{when } T_{h_r} \leq 0 \qquad (33)$$

Here also an effective speed of the rudder through the water of about 0.8 V_B is assumed. Again, the case that $T_{hr} \leq 0$ corresponds to the situation when the top of the rudder is above the water surface at the angle of heel θ. Also, the effective value of $(1 + T_{hr}/T_r)^2$ is equal to unity in that case since no side force is induced on the hull by the keel and no extra side force is induced on the rudder by the hull. The definition of the various entities in equations 29 through 33 is shown in Fig. 12b.

2.3 The Side Force on the Hull (Canoe Body)

The hull also experiences a side force at non-zero drift angles. Similarly to the procedures followed above, this side force can be written as:

$$L_{T_h} = \tfrac{1}{2}\rho V_B^2 \frac{\partial C_{L_h}}{\partial \beta} \cdot \beta \cdot A_h \cos\theta \qquad (34)$$

Since the effective aspect ratio of the hull is small (usually 0.30 or less), the theory of low aspect ratio wings (see for example Weinig [14]) can be applied, which leads to the result that the lift-curve slope of such a wing is equal to $\frac{\pi}{2} AR_h$. On applying this theory to the hull of a yacht it is assumed that the hull is modelled by a thin flat plate with the same (lateral) area and profile as the hull. Hoerner and Borst [3] show that this result is not correct due to the occurrence of a non-linear lift component equal to the force developed in the lift direction by drag. They give the following relation for the non-linear lift component for bodies with an aspect ratio of about 0.2:

$$\Delta C_{L_h} = 1.8 \sin^2\beta\cos\beta \qquad (35)$$

which, for drift angles less than about 10 degrees, leads to:

$$\Delta C_{L_h} \simeq 1.8\beta^2 \qquad (36)$$

It follows then that the lift-curve slope of the canoe body can be written as:

$$\frac{\partial C_{L_h}}{\partial \beta} = \left(\frac{\pi}{2}AR_h + 1.8\beta\right)(1+\Delta b/b)^2 \qquad (37)$$

Since the canoe body has a round "planform" and rounded "lateral edges" a value of -0.12 can be adopted for $\Delta b/b$ (see Table 1). Hence the following expression is obtained:

$$C_{L_h} = \frac{\partial C_{L_h}}{\partial \beta} \cdot \beta = 0.78\left(\frac{\pi}{2}AR_h + 1.8\beta\right)\beta \qquad (38)$$

and

$$L_{T_h} = \tfrac{1}{2}\rho V_B^2 \cdot 0.78(\pi T_h^2\cos\theta + 1.8A_h\beta)\beta\cos\theta \qquad (39)$$

where it is assumed that the effective aspect ratio of the hull (canoe body), at a heel angle θ, is approximately equal to $2T_h^2\cos\theta/A_h$, where T_h is the maximum draught of the canoe body and A_h the lateral area.

2.4 Side Force Calculations for 5.5 Metre Yacht "Antiope" and Comparisons with Results of Measurements

Measurements of the resistance and side force on the actual "Antiope" hull were carried out at the David Taylor Model Basin (now the David Taylor Naval Ship Research and Development Center) for the Technical and Research Panel H-13 (Sailing Yachts) of the Society of Naval Architects and Marine Engineers. The results of these measurements were presented by Herreshoff and Newman [15]. Resistance and side force measurements were carried out for various combinations of yaw angle β, rudder angle δ_r, heel angle θ and speed V_B. A lines drawing of "Antiope", taken from Letcher [16], is shown in Fig. 13. For the calculation of the side force on the keel and rudder (which is attached to the keel), the rudder can be considered as a trim tab so that equation 16 applies. From the data given in references 15 and 16 the following data, required for the calculations, were derived:

$T_{h_{ktt}}$ = 0.58 m
$T_{k_{tt}}$ = 1.41 m
Λ_{ktt} = 0.716 radians
$(t/c)_{ktt}$ = 0.07
$\tau_{T_{tt}}$ = 1.13x0.07=0.079
A_{tt}/A_{ktt} = 0.12
$\Lambda_{H_{tt}}$ = -0.54 radians
A_{ktt} = 1.90 m^2
A_h = 3.05 m^2

The aspect ratio is:

$$AR_{ktt}=\frac{2(1.41-0.58)^2\cos\theta}{1.90} = 0.725\cos\theta$$

The theoretical flap effectiveness ratio is:

$$\left(\frac{\partial\beta}{\partial\delta_{tt}}\right)_{th} = \frac{2}{\pi}\left(\sqrt{0.12(1-0.12)} + \arcsin\sqrt{0.12}\right)=0.432$$

and

$$\left(\frac{\partial\beta}{\partial\delta_{tt}}\right)_{o} = 0.432(0.75+0.25(0.12)^{0.1} +$$

$$-7.35(1-(0.12)^{0.1})\tan(0.079))\cos(-0.54) =$$

$$= 0.312. \text{ Thus:}$$

$$\frac{\partial\beta}{\partial\delta_{tt}} = 1-(1-0.312)\left(\sin\left(\frac{0.17\pi(0.725)\cos\theta}{2\times0.312}\right)\right)^{0.25}$$

$$= 1-0.688(\sin(0.621\cos\theta))^{0.25}$$

The two-dimensional lift-curve slope is:

$$a_{o_{ktt}} = 1+0.82(0.07)-\tan(0.079)\left(\frac{0.117}{0.07}+3.2(0.07)+\right.$$

$$\left.+\ 3.9(0.07)^2\right)=0.906$$

The keel has rounded lateral edges, so that $\Delta b/b=-0.09$. Hence:

$$\frac{\partial C_{L_{ktt}}}{\partial\beta} = \frac{2\pi(0.906)0.725\cos\theta(1-0.09)^2}{2(0.906)+\cos(0.716)\sqrt{\frac{(0.725\cos\theta)^2}{\cos^4(0.716)}+4}}$$

$$= \frac{3.418\cos\theta}{1.812+0.754\sqrt{1.622\cos^2\theta+4}}$$

The side force of keel and rudder (trim tab) is:

$$L_{T_{ktt}}=\tfrac{1}{2}\rho V_B^2\,\frac{3.418\cos\theta(\beta+(1-0.688)}{1.812+}$$

$$\frac{(\sin(0.621\cos\theta))^{0.25})\delta_{tt})(1+\frac{0.58}{1.41})^2 1.9\cos\theta}{+\ 0.754\sqrt{1.622\cos^2\theta+4}}$$

The side force of the canoe body is:

$$L_{T_h}=\tfrac{1}{2}\rho V_B^2(0.78)(\pi(0.58)^2\cos\theta+1.8(3.05)\beta)\beta\cos\theta$$

$$=\tfrac{1}{2}\rho V_B^2(0.824\beta\cos^2\theta+4.282\beta^2\cos\theta)$$

The results of the measurements, as presented by Letcher [16], are given as lift coefficients, using the upright projected lateral area (4.95 m^2) as the reference area. On following this example the following expression for the total side force coefficient is obtained:

$$C_{L_T} = \frac{C_L}{\tfrac{1}{2}\rho V_B^2 A_.} = \frac{2.613\ (\ \beta\ +}{1.812\ +}$$

$$\frac{+(1-0.688(\sin(0.621\cos\theta))^{0.25})\delta_{tt})\cos^2\theta}{+\ 0.754\sqrt{1.622\cos^2\theta+4}}\ +$$

$$+0.1665\beta\cos^2\theta\ +\ 0.8651\beta^2\cos\theta$$

Comparisons between calculated values according to this equation and Letcher's reduced data are made in Table 2. Only the measured data for which the standard deviation is less than 0.1 has been considered.

On not considering the comparisons for data points 5, 7, 13, 14 and 15, for which the measured values are probably subject to relatively large errors, the average absolute difference between measured and calculated values is about 4.9% which is sufficiently small for all practical purposes.

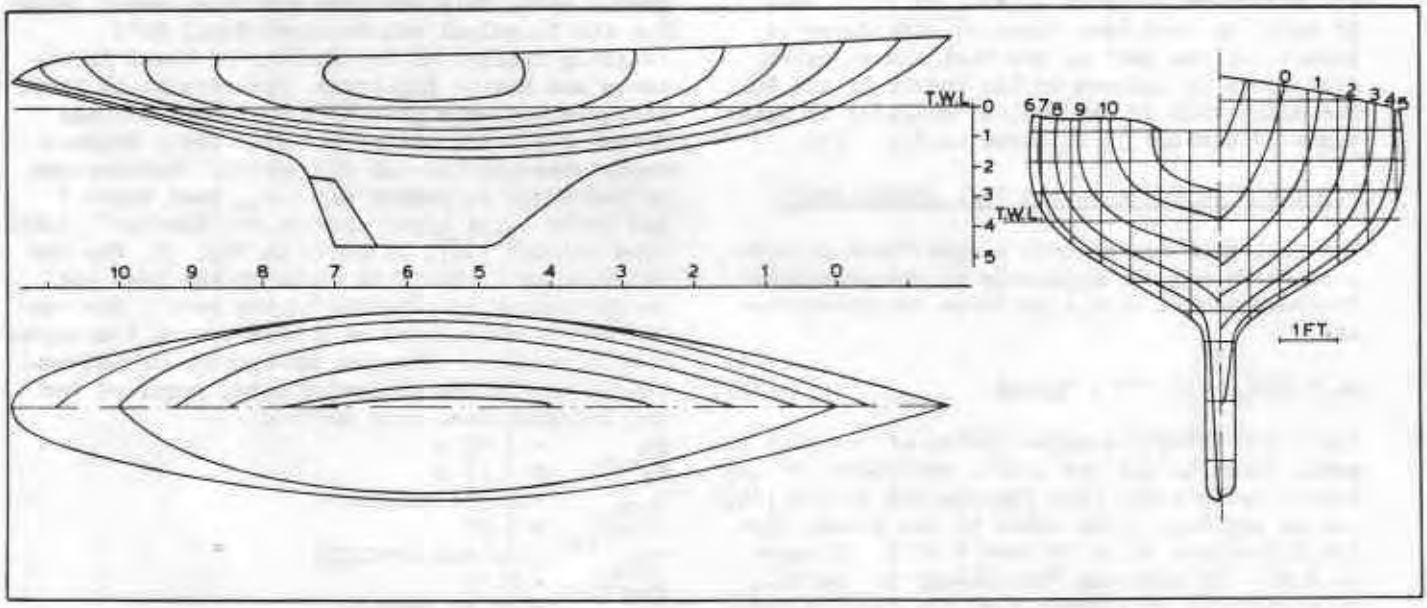

Fig. 13 Lines of "Antiope" showing the test waterline.

TABLE II Comparison between calculated and measured side force values for "Antiope"

Data point	heel angle	drift angle	rudder angle	measured side force	calculated side force
	θ^o	β^o	$\delta_{tt}{}^o$	$C_{L_T}x100$	$C_{L_T}x100$
1	0	0	0	0.14	0
2	1.0	2.70	0	4.56	4.40
3	3.0	2.74	0	4.71	4.45
4	5.0	2.79	0	4.80	4.52
5	20.0	3.15	0	3.99	4.61
6	21.5	3.19	0	4.94	4.58
7	22.8	3.22	0	5.23	4.55
8	21.4	7.01	0	10.72	10.74
9	23.3	7.05	0	10.27	10.55
10	25.9	7.11	0	10.30	10.26
11	13.0	6.82	0	11.40	11.31
12	19.6	6.97	0	11.70	10.90
13	9.0	0.22	0	0.01	0.34
14	9.3	0.23	0	0.50	0.35
15	9.5	0.23	0	0.79	0.35
16	10.1	2.92	3.0	6.34	6.12
17	11.0	2.95	3.0	6.44	6.14
18	14.6	3.03	3.0	6.66	6.11
19	10.4	2.94	6.0	7.82	7.62
20	16.1	3.07	6.0	7.98	7.53
21	10.9	2.94	1.6	5.91	5.43
22	12.3	2.98	1.6	6.09	5.45
23	14.2	3.02	1.6	6.20	5.44
24	10.2	2.92	0	4.78	4.63
25	13.8	3.01	0	5.12	4.67
26	11.3	2.95	3.0	5.89	6.13
27	14.7	3.03	3.0	6.27	6.11
28	6.9	6.67	0	11.52	11.41
29	10.4	6.76	0	12.00	11.39

3. CALCULATION OF THE HYDRODYNAMIC RESISTANCE

3.1 The Viscous Resistance

3.1.1 The Basic Equation for the Viscous Resistance

The total hydrodynamic resistance of a flat plate which is deeply submerged, at zero angle-of-attack, is equal to the frictional resistance R_{F_o} which can be written as:

$$R_{F_o} = C_{F_o} \tfrac{1}{2}\rho V^2 S \qquad (40)$$

where C_{F_o} = specific frictional resistance coefficient in a two-dimensional flow,
V = velocity of the plate through the fluid,
S = wetted area (of both sides) of flat plate.

This relation for the frictional resistance can also be adopted for the calculation of the frictional resistance of the hull, keel or rudder of a sailing yacht. In that case, however, R_{F_o} is not the total resistance, nor is it the total viscous resistance because, at the water surface, wavemaking occurs. For surface ships it is customary to divide the total resistance into a non-viscous part and a viscous part. The viscous resistance R_V is considered equivalent to the sum of the frictional resistance R_F of the three-dimensional hull (as distinct from R_{F_o} for a flat plate) and a pressure resistance component of viscous origin R_{PV}. The frictional resistance is associated with the force required to overcome the tangential stresses developed between the hull and the fluid, while the viscous pressure resistance is due to a pressure difference between the forebody and the aftbody of the hull. The growth of the boundary layer along the hull causes the pressure on the aftbody to be smaller than on the forebody leading to a resultant pressure force on the hull, of viscous origin, accordingly termed the viscous pressure resistance. Since R_{PV} is usually small, the viscous resistance is often written as:

$$R_V = C_V \tfrac{1}{2}\rho V^2 S \qquad (41)$$

where

$$C_V = C_{F_o}(1+k) \qquad (42)$$

in which C_V = specific total viscous resistance coefficient,
k = three-dimensional form factor on flat plate friction,
S = wetted surface of hull.

The form factor k thus accounts for the effects of the three-dimensional form on the value of C_{F_o} and for the viscous pressure resistance R_{PV}. From detailed boundary layer calculations carried out by Larsson for the 5.5 Metre Yacht "Antiope" [2], it is clear that for yacht-like hull forms, the effects of the form of the hull on the value of C_{F_o} is very small, and that the form factor mainly accounts for the viscous pressure resistance. Larsson found for a yacht speed of 3.05 m/sec that $C_F = 2.60 \times 10^{-3}$. According to equation 46 (see section 3.1.2), the flat plate value $C_{F_o} = 2.62 \times 10^{-3}$ when basing the calculation of the Reynolds number on an effective length of 0.8 L_{WL} (to account for the shorter length of the keel). It is assumed, therefore, that $C_F \approx C_{F_o}$ and that the form factor k approximately accounts for the effect of the viscous pressure resistance only.

In the calculation of the Reynolds number, an average hull length equal to 0.7 or 0.8 of the waterline length is usually adopted, following the practice of Davidson some 40 years ago [17]. In the last decade, however, the development in the design of keels and rudders of sailing yachts has been such that they can now be considered as appendages rather than as an integral part of the hull. Keels and rudders are now proportioned in accordance to their main function, as control surfaces. Since control surfaces become more effective as their aspect ratio increases, yacht keels and rudders are nowadays appreciably shorter. Also, rudders are now no longer placed immediately behind the keel, but at the aftermost part of the hull, where they are most effective. It follows that one particular value of the frictional resistance coeffi-

cient, based on an average value of the Reynolds number, cannot rightly reflect the considerable variation in length with draught of the underwater hull, keel and rudder of modern yachts. Obviously then, the best method to determine the viscous resistance of a sailing yacht is to perform the calculation of equation 42 separately for hull, keel and rudder, viz:

$$R_V=\tfrac{1}{2}\rho V_B^2(C_{F_h}(1+k_h)S_h+C_{F_k}(1+k_k)S_k+(0.8)^2C_{F_r}(1+k_r)S_r) \quad (43)$$

in which the subscripts h, k and r denote hull (canoe body), keel and rudder, respectively. The factor $(0.8)^2$ approximately accounts for the reduced speed of the flow relative to the rudder (see section 2.2.1).

3.1.2 The Frictional Resistance Coefficient

There is considerable evidence that the boundary layer along parts of the hull, keel or rudder of a sailing yacht can be laminar. Tanner [18] tank tested a full-scale International 10 Square Metre Class Canoe, fitted with six different centre-boards, from which he found that the boundary layer over the centre-boards was dominantly laminar. The Reynolds number of the centre boards (based on the average chord length) in the tests extended up to 9×10^5. Crago [19] noted that important extents of laminar flow exist along the hulls of sailing yachts "up to the size of a Dragon". It has been found that even larger yachts can "ghost" at 1 or 2 knots in absolutely calm conditions [20]. In a very comprehensive study on the significance of scale effects in resistance tests with sailing yacht models, Kirkman and Pedrick [21] conclude that laminar flow effects are very obvious up to Reynolds numbers of at least 1×10^6.

To account for the effects of laminar flow along the hull, keel or rudder, it is possible to adopt a formula for C_F such as was devised by Prandtl and Schlichting [22], viz:

$$C_F = C_{F_{turb}} - \frac{c}{R_n} \quad (44)$$

where $C_{F_{turb}}$ = skin friction coefficient for a turbulent boundary layer along a flat plate,
c = a constant,
R_n = Reynolds number.

From the results obtained by Gebers and Blasius [23] for the skin friction of flat plates with sharp leading edges, Prandtl concluded that laminar to turbulent transition began for $R_n=5\times10^5$ and that the skin friction coefficient assumed values according to fully turbulent flow at approximately 5×10^6. Accordingly, he adopted the following formula:

$$C_F=\frac{0.074}{(R_n)^{0.2}} - \frac{1700}{R_n} \quad (45)$$

which reflects the influence of laminar flow on C_F in the Reynolds number range between 5×10^5 and 5×10^6. On adopting the 1957 ITTC friction formulation for a turbulent boundary layer, the same influence of laminar flow is obtained when the following equation is used:

$$C_F=\frac{0.075}{(\log_{10}R_n-2)^2} - \frac{1800}{R_n} \quad (46)$$

Values according to equation 45 are shown in Fig. 14. For flat plates with rounded leading edges, Wieselsberger [24] and others have found that the value of the skin friction coefficient reflects the existence of a turbulent flow down to a Reynolds number of 1×10^5. Subsequent studies have revealed that this is caused by early transition, due to the existence of an adverse pressure gradient just downstream of the rounded leading edge. Such adverse pressure gradients do not occur, however, so close to the leading edges of keels and rudders normally applied, at angles-of-attack less than about 7 degrees. Accordingly, equation 46 would seem to be applicable for the calculation of realistic C_F-values for the hull, keel and rudder of sailing craft, when hydrodynamically smooth, for Reynolds number values in excess of 5×10^5. The Reynolds number to be used in combination with equation 46 is defined as:

$$R_{n_h} = \frac{V_B L_{WL}}{\nu} \quad (47)$$

$$R_{n_k} = \frac{V_B \bar{c}_k}{\nu} \quad \text{and} \quad (48)$$

$$R_{n_r} = \frac{0.8 V_B \bar{c}_r}{\nu} \quad (49)$$

where the factor 0.8 in equation 49 approximately accounts for the decreased velocity of the flow to the rudder (see section 2.2.1). The kinematic viscosity ν of sea water equals 1.191×10^{-6} m^2/sec at 15°C. For some other water temperatures, the corresponding values are given in Table 3 for both sea water and fresh water.

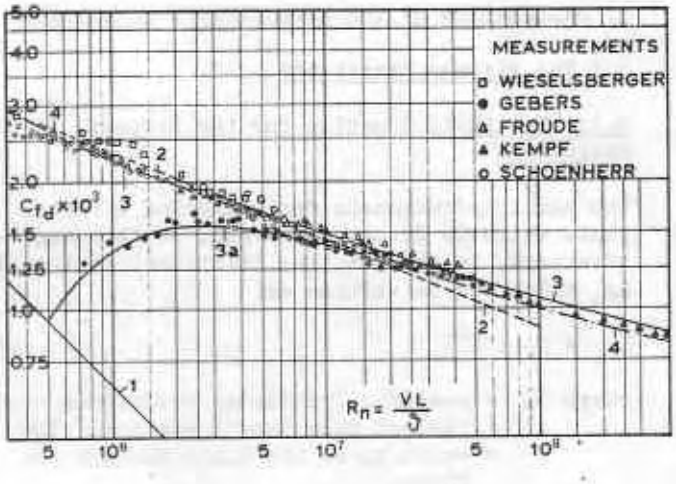

Fig. 14 Theoretical and measured values of the fictional resistance coefficient of smooth flat plates C_{F_0}. Theoretical curves are: 1, laminar (Blasius); 2, turbulent (Prandtl); 3, turbulent (Prandtl-Schlichting); 3a, transition laminar-turbulent (Prandtl-Schlichting); 4, turbulent (Schultz-Grunow). Equation 4/5 corresponds to curves 3 and 3a (from Ref. 7).

TABLE III Value of the kinematic viscosity ν at various temperatures for sea water and fresh water

Temp. (^{o}C)	Kinematic viscosity for sea water (m^2/sec)	Kinematic viscosity for fresh water (m^2/sec)
5	1.565×10^{-6}	1.519×10^{-6}
10	1.356×10^{-6}	1.308×10^{-6}
15	1.191×10^{-6}	1.142×10^{-6}
20	1.056×10^{-6}	1.007×10^{-6}
25	0.9458×10^{-6}	0.8965×10^{-6}
30	0.8528×10^{-6}	0.8045×10^{-6}

3.1.3 The Form Factor of Hull, Keel and Rudder

The form factor, as defined in equation 42, accounts for the increase in viscous resistance of a three-dimensional form (hull, keel or rudder) over that of a flat plate, with the same wetted area. In the method outlined in reference 1, the author adopted the form factor formula derived by Holtrop [25] for the canoe body. Larsson [2] found that this formula resulted in a value which was too high for "Antiope" (the formula gives a value of 1.23, while Larsson's results indicate a value of about 1.07). Since more accurate formulae for the form factor are not available it is more appropriate not to adopt the form factor concept for the canoe body and to use the flat plate approximation to the viscous resistance. The effect of not incorporating a form factor for the canoe body will not influence the result for the total resistance because in the calculation of the wave resistance (see section 3.2.1) an approach is used based on the residual resistance R_R, as obtained from towing tank measurements by subtraction of the equivalent flat plate frictional resistance R_{F_o} from the total resistance R_T, i.e. $R_R=R_T-R_{F_o}$. It follows that the viscous pressure resistance R_{PV}, being the difference between R_V and R_F, is included in this R_R-value, as used in section 3.2.

The effect of thickness on the drag of typical keel and rudder sections has been studied by Hoerner [26]. He derived formulas for NACA 4-digit-type profiles (typical of rudder sections) and for NACA 63, 64 and 65 profiles (typical of keel sections) which, as an approximation, can be adopted as expressions for the form factor of the rudder and keel, respectively. These formulas are as follows:

$$k_k \simeq 1.2(t/c)_k + 70(t/c)_k^4 \qquad (50)$$

$$k_r \simeq 2(t/c)_r + 60(t/c)_r^4 \qquad (51)$$

where t/c is the effective (average) thickness-to-chord ratio.

3.1.4 An Approximate Equation for the Wetted Surface of the Hull

When the wetted surface of the canoe body is not known, it can be approximately deduced from a formula given by Holtrop [25], viz:

$$S_h=L_{WL}(2T_h+B_{WL})C_{\textcircled{x}}^{0.5}(0.4530+0.4425C_{B_h}-0.2862C_{\textcircled{x}}+ - 0.003467B_{WL}/T_h+0.3696C_{WP}) \qquad (52)$$

where L_{WL} = length of the design waterline,
T_h = maximum draught of canoe body,
B_{WL} = beam of the design waterline,
$C_{\textcircled{x}}$ = maximum section coefficient (for yacht hulls not necessarily the midship section coefficient) = $\dfrac{A_{\textcircled{x}}}{B_{WL}.T_h}$,
C_{B_h} = block coefficient of canoe body,
C_{WP} = waterplane coefficient = $\dfrac{A_{WP}}{L_{WL}.B_{WL}}$,
$A_{\textcircled{x}}$ = area of maximum section and
A_{WP} = area of design waterplane.

To demonstrate the accuracy of equation 52 the calculated value for "Antiope" can be compared with the actual value. According to Letcher [16], the total wetted surface of "Antiope" (including the keel) is 14.80 m^2. On subtracting the wetted surface of the keel, which is approximately equal to 3.8 m^2 (approximately 2 times the lateral area), the wetted surface of the canoe body is found to be approximately 11.0 m^2. With L_{WL}= 7.41 m, T_h=0.58 m, B_{WL}=1.75 m, $C_{\textcircled{x}}$= 0.567, C_{B_h}=0.306 and C_{WP}=0.691 (where $C_{\textcircled{x}}$, C_{B_h} and C_{WP} were obtained from the lines drawing provided by Letcher in reference 16 and reproduced here in Fig. 13), the wetted surface according to equation 52 is calculated to be 10.83 m^2 which is very close to the actual value of approximately 11.0 m^2.

3.1.5 The Final Equations for the Viscous Resistance

The final equations for the viscous resistance of a hull-keel-rudder configuration become as follows:

$$R_V=C_{F_h}\tfrac{1}{2}\rho V_B^2 S_h+C_{F_k}(1+k_k)\tfrac{1}{2}\rho V_B^2 S_k+C_{F_r}(1+k_r)\tfrac{1}{2}\rho(0.8V_B)^2 S_r \qquad (53)$$

where

$$C_{F_{h,k,r}}=\frac{0.075}{(\log_{10}R_{n_{h,k,r}}-2)^2}-\frac{1800}{R_{n_{h,k,r}}} \qquad (46)$$

in which $R_{n_{h,k,r}}$ follow from equations 47, 48 and 49, respectively. If required, the wetted surface of the canoe body S_h can be determined approximately from equation 52. The form factors k_k and k_r follow from equations 50 and 51, respectively, while the wetted areas S_k and S_r are approximately:

$$S_k = 2(T_k-T_{h_k})\bar{c}_k \quad \text{and} \qquad (54)$$

$$S_r = 2(T_r-T_{h_r})\bar{c}_r \qquad (55)$$

3.3 The Induced Resistance

3.3.1 The Basic Equation for the Induced Resistance

Lift is generated by deflecting a flow over an angle α_i downward (or sideways) from its undisturbed direction. The force generated by the body which induces (deflects) this flow is directed at approximately right angles to the direction of the deflected flow, as shown in Fig. 15. It follows that the component of this force, F sin α_i, then acts against the direction of motion. This force is called the induced drag force R_I, because it is associated with the induced flow field. From Fig. 15 it follows that $R_I = F \sin \alpha_i = L \tan \alpha_i$. Hence $C_{R_I} = C_L \tan \alpha_i$. It can be shown that the induced flow angle α_i is related to the lift coefficient and the aspect ratio according to:

$$\alpha_i = \frac{C_L}{\pi AR} \qquad (60)$$

$$\text{therefore, } C_{R_I} = \frac{C_L^2}{\pi AR} \qquad (61)$$

since for small α_i-angles, $C_{R_I} \approx C_L \alpha_i$. Use of equation 2 (for a keel) together with $R_{I_k} = \frac{1}{2}\rho V_B^2 C_{R_I} A_k \cos\theta$, leads to:

$$R_{I_k} = \tfrac{1}{2}\rho V_B^2 \frac{C_{L_k}^2}{\pi AR_k} A_k \cos\theta = \frac{L_{T_k}^2}{\tfrac{1}{2}\rho V_B^2 A_k \cos\theta . \pi AR_k} \qquad (62)$$

where L_{T_k} follows from equation 13.

The induced resistance of a sailing yacht can then be determined on adding the induced resistance of the hull, keel (and trim tab) and rudder (and skeg), as follows:

$$R_{I_T} = \frac{2}{\rho V_B^2}\left(\frac{L_{T_h}^2}{\pi A_h \cos\theta . AR_h} + \frac{L_{T_k}^2}{\pi A_k \cos\theta . AR_k} + \frac{L_{T_r}^2}{(0.8)^2 \pi A_r \cos\theta . AR_r}\right) \qquad (63)$$

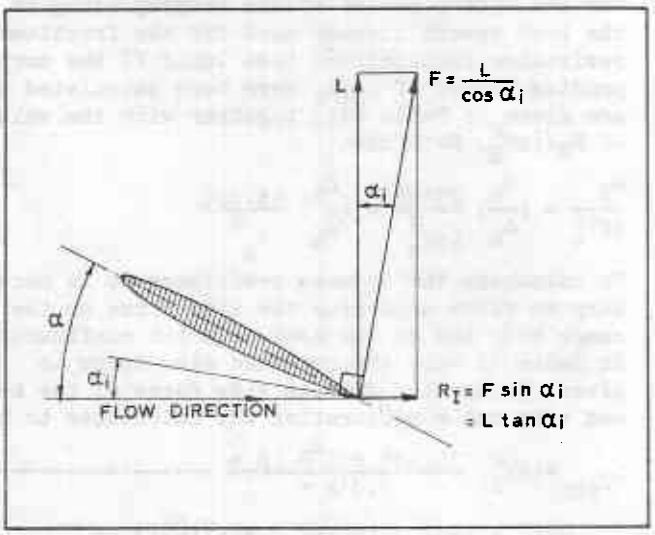

Fig. 15 Induced drag: a component of the lift force.

where L_{T_h}, L_{T_k} and L_{T_r} follow from equations 39, 13 and 29, respectively.

3.3.2 Effects of Planform and Sweep Angle of Keel and Rudder on Induced Resistance

Equation 60 is strictly only valid for an elliptical lift distribution over the span of the lifting surface. The planforms of present-day keels and rudders rarely lead to an elliptical spanwise loading, however. Appreciable increments in induced drag are found in planforms that are either extremely tapered or close to a rectangular shape. For taper ratios between 0.3 and 0.4, an elliptical spanwise loading is nearly obtained. In that case the additional induced drag is very small (about 1 or 2%). For other values of the taper ratio the following expression can be used, which fits the results given by Hoerner [26]; the expression itself is valid for the keel:

$$R_{I_k} = \frac{2}{\rho V_B^2}\left(\frac{L_{T_k}^2}{\pi A_k \cos\theta . AR_k}\right)\left(1 + (0.012 - 0.057\lambda_k + 0.095\lambda_k^2 - 0.040\lambda_k^3) AR_k\right) \qquad (64)$$

where $\lambda_k = \frac{C_{tip}}{C_{root}}$

with C_{tip} = chord length of the keel at the tip (bottom), and
C_{root} = chord length of the keel at the hull-keel intersection.

It should be noted that whereas elliptical or rounded planforms might be advantageous in minimizing induced drag, they also lead to a reduction in the total lift. As discussed in section 2.1.3, the effective span of rounded planforms is less than that of rectangular planforms. A consequence of this fact is that rectangular planforms often lead to the highest lift to drag ratios.

The effect of sweep is to increase the loading near the tip of the lifting surface. According to Hoerner [26], a sweep-back angle of 30° requires a taper ratio of about 0.15 to obtain near-elliptical loading (instead of about 0.35 for zero sweep-back). Since such taper ratios are rarely practical (except in delta configurations) it follows that the spanwise loading of swept-back lifting surfaces is not often near-elliptical, leading to somewhat higher induced drag values. Also, the lift force of each chordwise segment of the lifting surface approaching the tip is tilted further "backward" because of an increasing deflection of the induced flow, leading to larger flow angles α_i (see Fig. 15). It follows that because of this the component of the lift in the direction of the undisturbed flow becomes greater with increasing sweep back. According to Hoerner [26] the induced drag increases proportionally with sweep angle according to $1/\cos\Lambda$, where Λ is the sweep back (or forward) angle of the quarter-chord line of the lifting surface. Such an increase in induced drag, however, is never found in experimental sailing yacht studies. It would appear that the increase

in induced drag due to sweep is nearly completely compensated for by the favourable influence of sweep on the wave resistance [10]. The final expression for the induced resistance (for the keel) is therefore assumed to be given by equation 64.

3.3.3 The Final Equations for the Induced Resistance

For a keel-trim tab and skeg-rudder configuration, the total induced resistance can be written as:

$$R_{I_T} = R_{I_{ktt}} + R_{I_{sr}} + R_{I_h} \qquad (65)$$

where

$$R_{I_{ktt}} = \frac{2}{\rho V_B^2}\left(\frac{L_{T_{ktt}}^2}{\pi A_{ktt}\cos\theta.AR_{ktt}}\right)\left(1+\left(0.012 - 0.057\lambda_{ktt}+0.095\lambda_{ktt}^2-0.040\lambda_{ktt}^3\right)AR_{ktt}\right) \qquad (66)$$

$$R_{I_{sr}} = \frac{2}{\rho(0.8V_B)^2}\left(\frac{L_{T_{sr}}^2}{\pi A_{sr}\cos\theta.AR_{sr}}\right)\left(1+\left(0.012 - 0.057\lambda_{sr}+0.095\lambda_{sr}^2-0.040\lambda_{sr}^3\right)AR_{sr}\right) \qquad (67)$$

and

$$R_{I_h} = \frac{2}{\rho V_B^2}\left(\frac{L_{T_h}^2}{\pi A_h\cos\theta.AR_h}\right) \qquad (68)$$

In the induced resistance calculation for the hull (i.e. the canoe body), the effects of taper are neglected. The values for $L_{T_{ktt}}$, $L_{T_{sr}}$ and L_{T_h} follow from equation 16, 21 and 39. When a trim tab is not fitted to the keel, or when $\delta_{tt}=0$, the induced resistance of the keel becomes as given by equation 64. For the case of a rudder alone (without a skeg), the induced resistance of the rudder is:

$$R_{I_r} = \frac{2}{\rho(0.8V_B)^2}\left(\frac{L_{T_r}^2}{\pi A_r\cos\theta.AR_r}\right)\left(1+\left(0.012 - 0.057\lambda_r+0.095\lambda_r^2-0.040\lambda_r^3\right)AR_r\right) \qquad (69)$$

3.4 Resistance Calculations for 5.5 Metre Yacht "Antiope" and Comparisons with Results of Measurements

From the data given in references 15 and 16 the following values, required for the calculations, were derived:

L_{WL} = 7.41 m) L_{WL}/B_{WL} = 4.23
B_{WL} = 1.75 m) B_{WL}/T_h = 3.02
T_h = 0.58 m
C_{B_h} = 0.306
∇_h = 2.30 m^3
Δ_h = 2.3x1025x9.81 N = 23127 N
$C_{\mathbb{X}}$ = 0.567
C_{P_h} = 0.54
C_{WP} = 0.691
LCB = -2.2
i_E = 20°; C_{WL} = 20 x 4.23 = 84.6
A_h = 3.05 m^2
S_h = 14.80 - 3.80 = 11.0 m^2
A_{ktt} = 1.90 m^2
S_{ktt} = 3.80 m^2
T_{ktt} = 1.41 m
c_{ktt} = (3.03+1.61)/2 = 2.32 m
$(t/c)_{ktt}$ = 0.16/2.32 = 0.07
λ_{ktt} = 1.61/3.03 = 0.531
ν = 1.003x10^{-6} m^2/sec

The values of the Froude and Reynolds numbers, based on the waterline length of 7.41 m, for speeds of 2, 3, 4, 5, 6, and 6,5 knots (at which the measurements were carried out) have been calculated by Letcher [16]. Using these R_n-values, the frictional resistance coefficients of the hull can be calculated by means of equation 46. The frictional resistance coefficients of the keel, based on an average length of the keel of 2.32 m, can be calculated in the same manner. The form factor of the keel and rudder configuration (the rudder is again considered to be a trim tab) is:

$k_{ktt} = 2(0.07) + 60(0.07)^4 = 0.1414$ so that

$$R_F = \tfrac{1}{2}\rho V_B^2\left(C_{F_h}\times 11 + C_{F_{ktt}}\times 1.1414\times 3.8\right)$$

The results of the calculations for C_{F_h}, $C_{F_{ktt}}$ and R_F are given in Table V. The calculation of the wave resistance can best be started by first determining the values of C_1, C_2, C_3 and C_4 in equation 56. This is carried out by multiplying the values of the coefficients a_o through a_{11} (given in Table IV) by the values of LCB, LCB^2, C_{P_h}, etc., as prescribed by equation 58. The results of these multiplications are given in Table VI. Also, $m = 0.1435(0.54)^{-2.198} = 0.5560$.

Hence,

$$\frac{R_R}{\Delta_h} = 0.003709e^{-0.06177F_n^{-2}} + 0.550524e^{-0.556F_n^{-2}} + 0.182252\sin(F_n^{-2})e^{-0.556F_n^{-2}} + 0.037332\cos(F_n^{-2})e^{-0.556F_n^{-2}}$$

For the Froude number values corresponding to the boat speeds already used for the frictional resistance calculations (see Table V) the corresponding values of R_R/Δ_h have been calculated and are given in Table VII, together with the values of $R_R/\frac{1}{2}\rho V_B^2$. Note that:

$$\frac{R_R}{\frac{1}{2}\rho V_B^2} = \left(\frac{R_R}{\Delta_h}\right)\frac{23127}{\frac{1}{2}\rho V_B^2} = \left(\frac{R_R}{\Delta_h}\right)\frac{45.126}{V_B^2}$$

To calculate the induced resistance it is necessary to first determine the side force on the canoe body and on the keel-trim tab configuration. In Table II only the combined side force is given. In section 2.4 the side force of the keel and trim tab configuration was calculated to be:

$$L_{T_{ktt}} = \tfrac{1}{2}\rho V_B^2.\frac{12.936\cos^2\theta\,(\beta + \dfrac{+(1-0.688(\sin(0.621\cos\theta))^{0.25})\delta_{tt})}{1.812 + 0.754\sqrt{1.622\cos^2\theta + 4}}}$$

TABLE V Results of frictional resistance calculations for "Antiope"

V_B(knots)	2	3	4	5	6	6.5
V_B (m/sec)	1.029	1.543	2.058	2.572	3.086	3.344
$R_{n_h} x10^{-6}$	7.60	11.4	15.2	19.0	22.8	24.7
$C_{F_h} x10^{3}$	2.91	2.77	2.67	2.60	2.53	2.51
$R_{n_{ktt}} x10^{-6}$	2.38	3.57	4.76	5.95	7.14	7.73
$C_{F_{ktt}} x10^{3}$	3.16	3.11	3.05	2.99	2.93	2.91
$\frac{R_F}{\frac{1}{2}\rho V_B^2}$	0.0457	0.0440	0.0426	0.0416	0.0405	0.0402

TABLE VI Values of the terms in equation 58 for "Antiope"

Term	$C_1 x10^3$	$C_2 x10^3$	$C_3 x10^3$	$C_4 x10^3$
a_o	79.321	6714.9	-908.44	3012.1
a_1LCB	0.204	- 43.626	- 5.559	- 5.972
a_2LCB^2	- 0.010	12.923	- 1.732	1.235
$a_3 C_{P_h}$	-133.088	-10617.480	407.803	-4967.352
$a_4 C_{P_h}^2$	54.569	4111.560	- 14.271	2008.133
$a_5 L_{WL}/B_{WL}$	- 6.044	580.948	41.745	- 676.504
$a_6 (L_{WL}/B_{WL})^2$	2.129	- 239.210	- 13.894	290.509
$a_7 C_{WL}$	13.305	- 380.573	320.651	- 69.384
$a_8 C_{WL}^2$	- 4.581	150.300	-134.483	16.104
$a_9 B_{WL}/T_h$	- 7.636	653.679	- 27.917	713.868
$a_{10} (B_{WL}/T_h)^2$	4.617	- 319.907	11.726	- 402.921
$a_{11} C_{\textcircled{a}}$	0.923	- 72.990	142.119	117.516
	3.709	550.524	-182.252	37.332

TABLE VII Results of residual resistance calculations for "Antiope"

V_B(knots)	2	3	4	5	6	6.5
V_B(m/sec)	1.029	1.543	2.058	2.572	3.086	3.344
F_n	0.121	0.181	0.241	0.301	0.361	0.392
R_R/Δ_h	0.0001	0.0006	0.0014	0.0027	0.0076	0.0171
$\frac{1}{2}\rho V_B^2$	542.7	1220.2	2170.6	3390.3	4880.7	5730.9
$R_R/\frac{1}{2}\rho V_B^2$	0.0006	0.0106	0.0133	0.0182	0.0361	0.0692

TABLE IX Comparison between calculated and measured resistance for "Antiope"

Data point	speed (knots) V_B	heel angle θ^o	drift angle β^o	rudder angle δ_{tt}^o	$\frac{R_F}{\frac{1}{2}\rho V_B^2 A}$	$\frac{R_W}{\frac{1}{2}\rho V_B^2 A}$	$\frac{R_{I_T}}{\frac{1}{2}\rho V_B^2 A}$	$\frac{R_T}{\frac{1}{2}\rho V_B^2 A}$	$\frac{R_T}{\frac{1}{2}\rho V_B^2 A} \times 10^2$
					CALCULATED ($\times 10^2$)				MEASURED
1	5	0	0	0	0.840	0.368	0	1.21	1.28
2	4	1.0	2.70	0	0.861	0.269	0.156	1.29	1.26
3	5	3.0	2.74	0	0.840	0.369	0.160	1.37	1.41
4	6	5.0	2.79	0	0.818	0.734	0.166	1.72	1.85
5	2	20.0	3.15	0	0.923	0.014	0.194	1.13	1.11
6	5	21.5	3.19	0	0.840	0.425	0.194	1.46	1.44
7	6	22.8	3.22	0	0.818	0.857	0.196	1.87	1.97
8	3	21.4	7.01	0	0.889	0.247	1.036	2.17	1.86
9	4	23.3	7.05	0	0.861	0.319	1.030	2.21	1.83
10	5	25.9	7.11	0	0.840	0.455	1.012	2.31	1.96
11	4	13.0	6.82	0	0.861	0.283	1.051	2.19	1.84
12	6	19.6	6.97	0	0.818	0.821	1.044	2.68	2.63
13	2	9.0	0.22	0	0.923	0.013	0.002	0.94	1.20
14	5	9.3	0.23	0	0.840	0.378	0.002	1.22	1.31
15	6	9.5	0.23	0	0.818	0.749	0.004	1.57	1.68
16	3	10.1	2.92	3.0	0.889	0.221	0.331	1.44	1.30
17	4	11.0	2.95	3.0	0.861	0.279	0.333	1.47	1.36
18	6	14.6	3.03	3.0	0.818	0.778	0.341	1.94	1.95
19	3	10.4	2.94	6.0	0.889	0.222	0.537	1.65	1.46
20	6	16.1	3.07	6.0	0.818	0.789	0.546	2.15	2.08
21	4	10.9	2.94	1.6	0.861	0.279	0.255	1.39	1.33
22	5	12.3	2.98	1.6	0.840	0.385	0.261	1.49	1.51
23	6	14.2	3.02	1.6	0.818	0.775	0.263	1.86	1.93
24	3	10.2	2.92	0	0.889	0.221	0.178	1.29	1.20
25	6	13.8	3.01	3.0	0.818	0.772	0.186	1.78	1.86
26	4	11.3	2.95	3.0	0.861	0.280	0.333	1.47	1.32
27	6	14.7	3.03	0	0.818	0.779	0.341	1.94	1.94
28	5	6.9	6.67	0	0.840	0.373	1.030	2.24	1.99
29	6	10.4	6.76		0.818	0.753	1.047	2.62	2.53

TABLE X Comparison between calculated and measured resistance for "Antiope" for zero heel, drift and rudder angles

Data point	speed (knots) V_B	heel angle θ^o	drift angle β^o	rudder angle δ_{tt}^o	$\frac{R_F}{\frac{1}{2}\rho V_B^2 A}$	$\frac{R_W}{\frac{1}{2}\rho V_B^2 A}$	$\frac{R_{I_T}}{\frac{1}{2}\rho V_B^2 A}$	$\frac{R_T}{\frac{1}{2}\rho V_B^2 A}$	$\frac{R_T}{\frac{1}{2}\rho V_B^2 A} \times 10^2$
					CALCULATED ($\times 10^2$)				
30	2	0	0	0	0.923	0.013	0	0.94	1.06
31	3	0	0	0	0.889	0.214	0	1.10	1.04
32	4	0	0	0	0.861	0.269	0	1.13	1.12
33	5	0	0	0	0.840	0.368	0	1.21	1.28
34	6	0	0	0	0.818	0.728	0	1.55	1.67
35	6.5	0.1	0	0	0.812	1.397	0	2.21	2.23

TABLE VIII Calculation of the induced resistance for "Antiope"

Data point	heel angle θ^o	drift angle β^o	rudder angle δ_{tt}^o	$\frac{L_{T_{ktt}}}{\frac{1}{2}\rho V_B^2}$	$\frac{L_{T_h}}{\frac{1}{2}\rho V_B^2}$	$\frac{R_{I_{ktt}}}{\frac{1}{2}\rho V_B^2}$	$\frac{R_{I_h}}{\frac{1}{2}\rho V_B^2}$	$\frac{R_{I_T}}{\frac{1}{2}\rho V_B^2}$
1	0	0	0	0	0	0	0	0
2	1.0	2.70	0	0.1693	0.0483	0.0066	0.0011	0.0077
3	3.0	2.74	0	0.1714	0.0491	0.0068	0.0011	0.0079
4	5.0	2.79	0	0.1737	0.0499	0.0070	0.0012	0.0082
5	20.0	3.15	0	0.1759	0.0522	0.0081	0.0015	0.0096
6	21.5	3.19	0	0.1749	0.0521	0.0081	0.0015	0.0096
7	22.8	3.22	0	0.1735	0.0518	0.0082	0.0015	0.0097
8	21.4	7.01	0	0.3848	0.1471	0.0395	0.0118	0.0513
9	23.3	7.05	0	0.3773	0.1451	0.0391	0.0119	0.0510
10	25.9	7.11	0	0.3659	0.1421	0.0383	0.0118	0.0501
11	13.0	6.82	0	0.4076	0.1522	0.0405	0.0115	0.0520
12	19.6	6.97	0	0.3911	0.1487	0.0399	0.0118	0.0517
13	9.0	0.22	0	0.0135	0.0031	0.0001	0	0.0001
14	9.3	0.23	0	0.0141	0.0033	0.0001	0	0.0001
15	9.5	0.23	0	0.0141	0.0033	0.0001	0.0001	0.0002
16	10.1	2.92	3.0	0.2512	0.0517	0.0151	0.0013	0.0164
17	11.0	2.95	3.0	0.2519	0.0520	0.0152	0.0013	0.0165
18	14.6	3.03	3.0	0.2502	0.0524	0.0155	0.0014	0.0169
19	10.4	2.94	6.0	0.3252	0.0520	0.0253	0.0013	0.0266
20	16.1	3.07	6.0	0.3200	0.0526	0.0256	0.0014	0.0270
21	10.9	2.94	1.6	0.2172	0.0518	0.0113	0.0013	0.0126
22	12.3	2.98	1.6	0.2177	0.0522	0.0115	0.0014	0.0129
23	14.2	3.02	1.6	0.2170	0.0524	0.0116	0.0014	0.0130
24	10.2	2.92	0	0.1778	0.0516	0.0075	0.0013	0.0088
25	13.8	3.01	0	0.1788	0.0523	0.0078	0.0014	0.0092
26	11.3	2.95	3.0	0.2513	0.0519	0.0152	0.0013	0.0165
27	14.7	3.03	3.0	0.2500	0.0524	0.0155	0.0014	0.0169
28	6.9	6.67	0	0.4127	0.1521	0.0399	0.0111	0.0510
29	10.4	6.76	0	0.4111	0.1527	0.0404	0.0114	0.0518

TABLE IX Comparison between calculated and measured resistance for "Antiope"

Data point	speed (knots) V_B	heel angle θ^o	drift angle β^o	rudder angle δ_{tt}^o	$\frac{R_F}{\frac{1}{2}\rho V_B^2 A}$	$\frac{R_W}{\frac{1}{2}\rho V_B^2 A}$	$\frac{R_{I_T}}{\frac{1}{2}\rho V_B^2 A}$	$\frac{R_T}{\frac{1}{2}\rho V_B^2 A}$	$\frac{R_T}{\frac{1}{2}\rho V_B^2 A} \times 10^2$
					CALCULATED ($\times 10^2$)				MEASURED
1	5	0	0	0	0.840	0.368	0	1.21	1.28
2	4	1.0	2.70	0	0.861	0.269	0.156	1.29	1.26
3	5	3.0	2.74	0	0.840	0.369	0.160	1.37	1.41
4	6	5.0	2.79	0	0.818	0.734	0.166	1.72	1.85
5	2	20.0	3.15	0	0.923	0.014	0.194	1.13	1.11
6	5	21.5	3.19	0	0.840	0.425	0.194	1.46	1.44
7	6	22.8	3.22	0	0.818	0.857	0.196	1.87	1.97
8	3	21.4	7.01	0	0.889	0.247	1.036	2.17	1.86
9	4	23.3	7.05	0	0.861	0.319	1.030	2.21	1.83
10	5	25.9	7.11	0	0.840	0.455	1.012	2.31	1.96
11	4	13.0	6.82	0	0.861	0.283	1.051	2.19	1.84
12	6	19.6	6.97	0	0.818	0.821	1.044	2.68	2.63
13	2	9.0	0.22	0	0.923	0.013	0.002	0.94	1.20
14	5	9.3	0.23	0	0.840	0.378	0.002	1.22	1.31
15	6	9.5	0.23	0	0.818	0.749	0.004	1.57	1.68
16	3	10.1	2.92	3.0	0.889	0.221	0.331	1.44	1.30
17	4	11.0	2.95	3.0	0.861	0.279	0.333	1.47	1.36
18	6	14.6	3.03	3.0	0.818	0.778	0.341	1.94	1.95
19	3	10.4	2.94	6.0	0.889	0.222	0.537	1.65	1.46
20	6	16.1	3.07	6.0	0.818	0.789	0.546	2.15	2.08
21	4	10.9	2.94	1.6	0.861	0.279	0.255	1.39	1.33
22	5	12.3	2.98	1.6	0.840	0.385	0.261	1.49	1.51
23	6	14.2	3.02	1.6	0.818	0.775	0.263	1.86	1.93
24	3	10.2	2.92	0	0.889	0.221	0.178	1.29	1.20
25	6	13.8	3.01	3.0	0.818	0.772	0.186	1.78	1.86
26	4	11.3	2.95	3.0	0.861	0.280	0.333	1.47	1.32
27	6	14.7	3.03	0	0.818	0.779	0.341	1.94	1.94
28	5	6.9	6.67	0	0.840	0.373	1.030	2.24	1.99
29	6	10.4	6.76		0.818	0.753	1.047	2.62	2.53

TABLE X Comparison between calculated and measured resistance for "Antiope" for zero heel, drift and rudder angles

Data point	speed (knots) V_B	heel angle θ^o	drift angle β^o	rudder angle δ_{tt}^o	$\frac{R_F}{\frac{1}{2}\rho V_B^2 A}$	$\frac{R_W}{\frac{1}{2}\rho V_B^2 A}$	$\frac{R_{I_T}}{\frac{1}{2}\rho V_B^2 A}$	$\frac{R_T}{\frac{1}{2}\rho V_B^2 A}$	$\frac{R_T}{\frac{1}{2}\rho V_B^2 A} \times 10^2$
					CALCULATED ($\times 10^2$)				
30	2	0	0	0	0.923	0.013	0	0.94	1.06
31	3	0	0	0	0.889	0.214	0	1.10	1.04
32	4	0	0	0	0.861	0.269	0	1.13	1.12
33	5	0	0	0	0.840	0.368	0	1.21	1.28
34	6	0	0	0	0.818	0.728	0	1.55	1.67
35	6.5	0.1	0	0	0.812	1.397	0	2.21	2.23

5. LIST OF SYMBOLS

A	Projected lateral area (one side only)
A_{WP}	Area of design waterplane
$A_{\otimes}$	Area of maximum section
AR	Effective aspect ratio ($=2b^2\cos\theta/A$)
AR_{geom}	Geometric aspect ratio ($=b^2/A$)
a_o	Two-dimensional lift-curve slope factor
B	Beam or breadth
B_{WL}	Beam of design waterline
b	Span (or depth) of a lifting surface
Δb	Effective reduction of span of a lifting surface due to a rounded planform and/or rounded lateral edges
C_B	Block coefficient ($\nabla_h/(L_{WL}.B_{WL}.T_h)$)
C_F	Frictional resistance coefficient of (three-dimensional) hull
$C_{F_{turb}}$	Frictional resistance coefficient of flat plate in turbulent boundary layer
C_{F_o}	Frictional resistance coefficient of equivalent flat plate
C_L	Lift coefficient
ΔC_{L_h}	Non-linear side force component on the canoe body
C_{L_T}	Lift coefficient of total hydrodynamic side force on yacht
C_M	Midship section coefficient
C_P	Prismatic coefficient ($\nabla_h/(A_{\otimes}L_{WL})$)
C_R	Residuary upright resistance coefficient
C_{R_I}	Induced resistance coefficient
C_V	Viscous resistance coefficient
C_{WL}	Half angle of entrance of waterline coefficient ($=i_E.L_{WL}/B_{WL}$)
C_{WP}	Waterplane coefficient ($A_{WP}/(L_{WL}.B_{WL})$)
$C_{\otimes}$	Maximum section coefficient ($A_{\otimes}/(B_{WL}.T_h)$)
c	Chord of a lifting surface
$\bar{c}$	Average (mean) chord of a lifting surface
c_{root}	Chord length of root section of a lifting surface
c_{tip}	Chord length of tip section of a lifting surface
F_n	Froude number based on waterline length ($=V/\sqrt{gL_{WL}}$)
g	Acceleration due to gravity ($=9.81$ m/sec^2)
h	Subscript denoting base hull (also termed "canoe body")
i_E	Half angle of entrance of design waterline in degrees
k	Form factor accounting for effect of three-dimensional form on viscous resistance, and subscript denoting keel
ktt	Subscript denoting combined keel and trim tab configuration
L	Length, and lift (or side force) of a lifting surface
ΔL_h	Side force increment induced on canoe body by keel
ΔL_k	Side force induced on keel due to cross flow on the hull
L_T	Total lift or side force on a lifting surface (including so-called wing-body effects)
LCB	Longitudinal centre of buoyancy relative to amidship in percent of L_{WL} (positive for positions in front of amidship)
L_{WL}	Length of waterline
R	Resistance force
R_F	Frictional resistance of (three-dimensional) hull
R_{F_o}	Frictional resistance of equivalent flat plate
R_I	Induced resistance (due to side force)
R_{I_T}	Total induced resistance
R_n	Reynolds number ($=V_B L_{WL}/\nu$ for hull)
R_{PV}	Viscous pressure resistance ($=R_V-R_F$)
R_R	Residuary resistance in upright condition
R_T	Total hydrodynamic resistance
R_V	Viscous resistance ($=R_F+R_{PV}$)
R_W	Wave resistance in heeled condition
r	Subscript denoting rudder
sr	Subscript denoting combined skeg and rudder configuration
S	Wetted surface area (both sides)
T	Draught
T_h	Maximum draught of canoe body
T_{h_k}	Average draught of canoe body at the location of the keel
$T_{h_{ktt}}$	Average draught of canoe body at the location of the keel-trim tab configuration
T_{h_r}	Average draught of canoe body at the location of the rudder
$T_{h_{sr}}$	Average draught of canoe body at the location of the skeg-rudder configuration
t/c	Average (mean) thickness to chord ratio of lifting surface
tt	Subscript denoting trim tab
V	Velocity or speed
V_B	Velocity of yacht through the water in the direction of heading
α	Angle-of-attack
α_i	Induced angle-of-attack
β	Drift or leeway angle (also termed yaw angle)
Δ	Displacement weight
∇	Volume of displacement
δ_r	Rudder deflection angle
δ_{tt}	Trim tab deflection angle
ϵ_T	Slope at the trailing edge of the average (mean) section of a lifting surface ($=\frac{\tan\tau_T}{t/c}$)
θ	Heel angle
λ	Taper ratio of a lifting surface
Λ	Sweep angle of quarter-chord line of a lifting surface
Λ_H	Sweep angle of hinge line of trim tab or rudder
ν	Kinematic viscosity of water
ρ	Density of water ($=1000$ kg/m^3 for fresh water and 1025 kg/m^3 for sea water)
τ_T	Half angle of trailing edge of the average (mean) section of a lifting surface
σ	Hull draught to keel (or rudder) draught ratio ($=T_{h_k}/T_k$ for keel)

6. LIST OF REFERENCES

1. Oossanen, P. van: "Theoretical Estimation of the Influence of Some Main Design Factors on the Performance of International Twelve Meter Class Yachts"; Fourth Chesapeake Sailing Yacht Symposium, Society of Naval Architects and Marine Engineers (Chesapeake Section), 1979.
2. Larsson, L.: "Theoretical Performance Predictions for the 5.5 Metre Yacht ANTIOPE"; Sixth Symposium on Yacht Architecture, under the auspices of the HISWA, 1979.
3. Hoerner, S.F. and Borst, H.V.: "Fluid-Dynamic Lift"; Hoerner Fluid Dynamics, 1975.
4. Whicker, L.F. and Fehlner, L.F.: "Free-Stream Characteristics of a Family of Low-Aspect Ratio, All-Movable Control Surfaces for Appli-

cation to Ship Design"; David Taylor Model Basin, Report No. 933, 1958.
5. Riegels, F.W.: "Aerofoil Sections", Butterworth & Co. Ltd., London, 1961.
6. Abbott, I.H. and Doenhoff, A.E. von: "Theory of Wing Sections"; Dover Publications, Inc., New York, 1959.
7. Schlichting, H. and Truckenbrodt, E.: "Aerodynamics of the Airplane"; McGraw-Hill International Book Co., New York, 1979.
8. Ashley, H. and Rodden, W.P.: "Wing-Body Aerodynamic Interaction"; Annual Review of Fluid Mechanics, Vol. 4, 1972.
9. Gerritsma, J.: "Course-Keeping Qualities and Motions in Waves of a Sailing Yacht"; Third AIAA Symposium on the Aerodynamics and Hydrodynamics of Sailing, 1971 (see also Delft Ship Hydromechanics Laboratory Report No. 200, 1968).
10. Beukelman, W. and Keuning, J.A.: "The Influence of Fin Keel Sweep-Back on the Performance of Sailing Yachts"; Fourth Symposium on Yacht Architecture, under the auspices of HISWA, 1975.
11. Flax, A.H.: "Simplification of the Wing-Body Problem"; Journal of Aeronautical Science, October 1973.
12. Vladen, : "Fuselage and Engine Nacelles Effects on Airplane Wings", NACA Technical Memorandum No. 736.
13. Glauert, H.: "Theoretical Relationship for an Aerofoil with Hinged Flap"; Aeronautical Research Council, London, Report and Memoranda 1095, 1927/1928.
14. Weinig, F.: "Beitrag zur Theorie des Tragflügels endlicher ins besondere kleiner Spannweite"; Deutsche Akademie der Luftfahrtforschung, Vol. 13, 1936 and Vol. 14, 1937 (see also NACA Technical Memoranda 1151, 1947).
15. Herreshoff, H.C. and Newman, J.N.: "Full-Scale Tank Tests of the 5.5 Metre Yacht ANTIOPE"; Society of Naval Architects and Marine Engineers, Technical and Research Bulletin No. 1-28, 1967.
16. Letcher, J.S.: "Sailing Hull Hydrodynamics, with Reanalysis of the ANTIOPE Data", Transactions of the Society of Naval Architects and Marine Engineers, Vol. 83, 1975.
17. Davidson, K.S.M.: "Some Experimental Studies of the Sailing Yacht", Transactions of the Society of Naval Architects and Marine Engineers, Vol. 44, 1936.
18. Tanner, T.: "Full-Scale Tank Tests of an International 10 Square Metre Class Canoe"; Transactions of the Royal Institution of Naval Architects, Vol. 102, 1960.
19. Crago, W.A.: "The Prediction of Yacht Performance from Tank Tests"; Transactions of the Royal Institution of Naval Architects, Vol. 105, 1963.
20. Gunning, M.F.: Written discussion to "The Prediction of Yacht Performance from Tank Tests "(see ref. 19); Transactions of the Royal Institution of Naval Architects, Vol. 105, 1963.
21. Kirkman, K.L. and Pedrick, D.R.: "Scale Effects in Sailing Yacht Hydrodynamic Testing"; Transactions of the Society of Naval Architects and Marine Engineers, Vol. 82, 1974.
22. Prandtl, L.: "The Mechanics of Viscous Fluids"; Division G of "Aerodynamic Theory", edited by Durand, W.F., Dover Publications, Inc., New York, 1963.
23. Schlichting, H.: "Boundary Layer Theory"; McGraw-Hill, New York, 1979.
24. Wieselsberger, C.: "Ergebnisse der Aerodynamischer Versuchsanstalt zu Göttingen"; Vol. 1 pp 121-126, Oldenbourg, Munich, 1935.
25. Holtrop, J. and Mennen, G.G.J.: "A Statistical Power Prediction Method"; International Shipbuilding Progress, 1978.
26. Hoerner, S.F.: "Fluid-Dynamic Drag"; Hoerner Fluid Dynamics, 1965.
27. Oossanen, P. van: "Resistance Prediction of Small, High-Speed Displacement Vessels: State-of-the-Art"; International Shipbuilding Progress, 1980.
28. Oortmerssen, G. van: "A Power Prediction Method and its Application to Small Ships"; International Shipbuilding Progress, 1971.
29. Havelock, T.H.: "The Wave-Making Resistance of Ships: A Theoretical and Practicle Analysis"; Proceeding of the Royal Society, A. Vol. 82 and Vol. 84, 1909.
30. Myers, H.A.: "Theory of Sailing Applied to Ocean Racing Yachts"; Marine Technology, July 1975.
31. Gerritsma, J., Moeyes, G. and Onnink, R.: "Test Results of a Systematic Yacht Hull Series"; Fifth Symposium on Yacht Architecture, under the auspices of HISWA, 1977.

A METHOD FOR THE CALCULATION OF RESISTANCE AND SIDE FORCE OF SAILING YACHTS

by Dr. P. Van Oossanen

DISCUSSION

S. NOUCHI (ENSM - Lab. D'Hydro Navale): I was surprised to see that you have used small boat formulae of the 1971 Oortmerssen paper. Why do you not use the systematic series of Gerritsma to get the co-efficients?

My second question is: is there a link between your theory and the MIT theory that was applied in the VVP prediction programme?

P. VAN OOSSANEN: The Delft series of model yachts are now nearing completion. As a matter of fact at a symposium in Amsterdam in August Professor Gerritsma will present the results of 16 systematic series of models, and the first nine are ready for publishing. However, these are typically IRR rates. In other words, the results will be very valid to use in IRR design. The hydrodynamics in this particular velocity prediction programme have to be a little more universal. We have had to come up with proper hydrodynamic modelling to cover the 10 low aspect ratio keel performance. However, we have ensured that the hydrodynamic model which we have used and derived fits closely the Delft results. There are a number of co-efficients in the formulae which have been tuned to fit a large amount of data, amongst which is this particular Delft series.

The programme adopts the MIT sail co-efficients . As a matter of fact we are now in the process of changing those co-efficients because at the New England symposium recently there was a paper in which the sail co-efficients were changed and are now more accurate. We have always used the Coleman and Newman sail co-efficients. However, the hydrodynamic modelling in the MIT velocity prediction programme is, in our opinion, a little inferior in that it only uses a number of results of a small number of model tests. They use the nine models of the Delft series and very little else. We were very concerned with the fact that the hydrodynamics involved there would not be sufficient to cover, for example, 12 metres, so we had to come up with something better. I feel that the programme we have is in a hydrodynamic sense a better one.

S. NOUCHI : The accuracy of your method you say is 4 per cent. Do you think this is enough for a 12 metre yacht?

P. VAN OOSSANEN: In this particular paper the results of full scale test with Antiope are used to give some hard numbers as to the ship method. The 4 per cent might disturb you because when you are dealing with 12 metres you are concerned about 1 per cent or ½ per cent, because that in itself will give you a major lead over your opponent. However, we use the programme only to ascertain in a qualitative sense the way in which the design should go. Then we do model tests to actually come down on a particular design with very specific numbers. So we use it in a qualitative sense for 12 metres. We use it in a qualitative sense for other types of yachts. We use it in a qualitative sense for 12 metres because there you are really looking at very minute details in performance.

P.J. BOLLEN (Bruntons Propellers Ltd); I do not know whether this is allowed under the 12 metre rule, but I would be interested to hear if any work is being done on the effect of filling out the ballast keel of a vessel of this nature to form a sort of analogy whith the wing fins on an aircraft.

P. VAN OOSSANEN: That I think would be allowed. You are certainly allowed to thicken the tip of the keel to a certain extent. However, you are talking about a yacht with displacement of 25 to 30 tons, of which the height of the keel is 1 metre to 1.2 metre. To be able to get in enough lead which would make a significant difference in that sense you would have to virtually go to a cylinder of something like 0.5 metre diameter, virtually covering up all the keel by the thickening which would do detriment, if it is sufficiently large, to its performance. In other words, simply bringing down the centre of gravity in this way will not give you that much benefit.

P.J. BOLLEN: I was thinking more of the possibility of putting a steel plate in this to reduce any loss of pressure.

P. VAN OOSSANEN: You are talking about hydrodynamic performance. The optimum shape of low aspect ratio keel configurations have been addressed in quite considerable detail. Unfortunately, most of the results are proprietary and will not be released. It would seem though that it is not the way to go. Any plate at the keel extremities would in itself have induced resistance.

P.G. SPENS: On that point, there have been model tests on various occasions at the Davidson

Laboratory trying end plates on the keel. It has never paid off. It has always put up the resistance.

DAVID MACKWORTH: As you probably know, there are a number of projects being bandied about for ships of between 200 and 600 tons having essentially commercial hull forms. Would it be reasonable to apply your equations to that sort of hull form

P. VAN OOSSANEN: Yes, by all means, particularly because with those sort of vessels you want to restrict draught to reasonable proportions so you have a very low aspect ratio under water appendages to the hull. The hydrodynamic equations in this particular computer model are applicable to this sort of vessel. As a matter of fact, we have used them to come up with performance predictions of a commercial sail type hull

A DELEGATE: I am not familiar with the hull forms used in your paper. Do they cover some form of block co-efficients in the commercial range.

P. VAN OOSSANEN: Very much so. As a matter of fact, that is what is so handsome about this particular model. The data population used to derive this particular equation is so very wide that you cannot go wrong unless you do very strange things.

A DELEGATE: To follow on from that, the additional residual resistance due to heel, I can see that as reasonable on basically a very round cance body, but that seems a little optimistic for a commercial type vessel with hard bilges.

P. VAN OOSSANEN: That is a valid point. Admittedly the co-sign square heel angle expression is one which was derived from racing hulltype forms We have done very little work on the effect of heel on the residual resistance of commercial type vessels. You are right. There would be a difference. This is something to be looked into. Mind you, I doubt whether the heel angles of commercial sailing vessels would be as big as those on racing craft, but the effect is still important enough to be looked at again.

A DELEGATE: You also deal with prediction of side force. Where you have residual heels the side force prediction is likely to fall within the same sort of percentage?

P. VAN OOSSANEN; Yes, there is a study we did. We did model tests as well which indicated that that was the case.

A DELEGATE: I have three questions. Have you any plans to include appendage drag on commercial sailing vessels, brackets, and so on.
Secondly, is there any experimental data to justify your assumption that the flow in the rudder was 0.8?
Thirdly, have you written a programme to do this particular prediction. If so, is it available commercially?

P. VAN OOSSANEN: We have looked at the appendage drag of propellers for 102 type boats. We have a lot of data on appendage drag on commercial vessels. Even though the paper does not describe a formula or an equation which you can use to account for that I am sure we could come up with something handsome. The model presented in the paper does not account for appendage drag other than skeg, rudders, keels etc.

We did a number of wake surveys on yachts at the location of the rudder to find out what sort of flow comes into the rudder. These were done on some very big models. We found that there are differences. It depends very much on drift angle The down wash, of course, increases as the drift angle increases. But on average, the 0.8 factor on 12 metres is quite good.

The programme is available without charge. It is on Algon and Fortran, and right now we are having someone writing it into Basic. It can be done on a pocket calculator in about three hours. For repeated use and in optimisation it has to be used time and time again. Hundreds of runs have to be made and a very small computer will suffice.

B.A. MORLEY (Australian Department of Defence [Navy]); Your estimations of trends in performance assume calm water. How valid is that for a wind speed of ---

P.VAN OOSSANEN: This is all calm water work. Data in seakeeping has not been released, but I would like to point out that the seakeeping work would indicate that if you are not looking at 6 inch. waterline but something like a foot, then the smaller boat has the best performance.

Let me just get that remark straight. You have to bear in mind the weather conditions and the sea conditions at Newport at the time. That is very difficult. You can find very little wave data around. As a matter of fact, the small boats around and the chop that they cause is a bigger problem. You are dealing with a lot of small waves, a sort of slapping type resistance phenomena. We did some modelling work on that and we feel that the so-called defraction effects which we had not accounted for might make the whole thing different. In other words, the work we did would seem to indicate that the results remained valid but it could be that some of the second order ship motion effects could change the results. Certainly, some people would support the idea that 44 feet waterline was too small because of this very effect.

B.A. MORLEY: You say you have done seakeeping calculations on 12 metres yachts and model tests. How good is the correlation?

P. VAN OOSSANEN: In motion it is pretty good. In added resistance we would have hoped the correlation was a little better. But in motions, which is important to see what sort of sail performance you can get, it was quite good.

THE CHAIRMAN: I have a small point to add on the 12 metre. I was heavily involved in writing the rules for the Alloy 12 several years ago. One of

the greatest difficulties was obtaining accurate data on previous 12s. The data published is very much different from the boats built.

P. VAN OOSSANEN: That is true, unfortunately.

WRITTEN DISCUSSION

Further contributions by Dr. P. Van Oossanen

S. NOUCHI: I was surprised to see the author use the small boat formulae of the 1971 Van Oortmerssen paper. I wish to ask him why he didn't use the results of the systematic series tested by Gerritsma. I would also like to enquire whether there is a link between the theory developed by the author and that developed at MIT for the so-called velocity prediction programme.
Is the accuracy of the method sufficient for predicting the performance of 12 Metre class yachts?

P. VAN OOSSANEN: Mr. Nouchi's comments relative to the use of Professor Gerritsma's systematic series results Ref. (1), in lieu of Van Oortmerssen's formulations are very valid.
At the coming HISWA symposium Ref (2) Professor Gerritsma will be presenting the results of the total series consisting of 22 yacht hull forms. These forms have all been developed from the "Standfast 43"designed by Frans Maas. The range of main dimensions of this series are as follows

$2.73 < L_{WL}/B_{WL} < 3.64$

$2.81 < B_{WL}/T_C < 5.35$

Corresponding values for yachts designed under the International Class Rule (5.5, 6 and 12 Metres) are: $L_{WL}/B_{WL} = 4.0$ and $B_{WL}/T_C = 2.40$.

It follows that the Delft series cannot be directly applied to the design and analysis of these yachts, for which the author has a special interest. The data base used by Van Oortmerssen, however, does include forms of comparable dimensions.

There is no link between the author's work and the so-called velocity prediction programme developed at M.I.T. The approach adopted by the author for the calculation of resistance and side force is essentially different, while at the present time also the adopted sail coefficient values are different. It is the intention, at a later stage perhaps, to adopt the sail coefficients as recently published by Hazen Ref. (3)

The results of the calculations for "Antiope" show that the author's method is not sufficiently accurate to predict resistance and side force to within about a 4 to 6 percent error. For 12 Metre Class Yachts, where performance differences of as much as 1 percent are significant, the method can only be used in a qualitative sense, for example for the prediction of the influence of a change in dimensions.

P. BOLLEN: I do not know whether this is allowed under the 12 Metre Class Rule, but I would be interested to hear if any work is being done on the effect of filling out the ballast keel of a vessel of this nature to form a sort of analogy with the wing fins on an aircraft to reduce any loss of pressure.

P. VAN OOSSANEN: The optimum shape of low aspect ratio keel configurations has been addressed in quite considerable detail. Unfortunately, most of the results are proprietary and cannot be released.

P.SPENS: On that point, there have been model tests on various occasions at the Davidson Laboratory trying end plates on the keel.It has never paid off. It has always put up the resistance.

D.MACKWORTH: As you probably know,there are a number of projects being bandied about for ships of between 200 and 600 tons having essentially commercial hull forms. Would it be reasonable to apply your equations to that sort of hull form?

P. VAN OOSSANEN: The data base, comprising some 1000 data points on which the used upright resistance formulations are based comprises a significant number of commercial hull forms. The formulations are valid for the following range of parameters.

$3.4 < L_{WL}/B_{WL} < 6.2$

$1.9 < B_{WL}/T_C < 3.6$

$0.5 < C_P < 0.72$

$0.7 < C_M < 0.96$

$-8.0\% L_{WL} < L_{CB} < +2\% L_{WL}$

A recent comparison of the author's upright resistance formulations with those of Gerritsma Ref(2) has shown that for $L_{WL}\ T_C/B_{WL}^2 < 1.0$ (which is the case for most types of yachts designed to the International Offshore Rule (IOR) the author's formulations are in error.

The resistance due to heel is assumed to vary with $1/\cos^2\theta$, where θ is the angle of heel. This seems to hold reasonably well for canoe bodies with basically a rounded shape.
The assumption is probably less valid for a commercial type vessel with hard bilges. It should be remembered, however, that the heel angle of commercial sailing ships will be much less than that of cruising and racing yachts.

The formulations for side force are also perhaps less valid for this type of hull form. No extensive study has yet been carried out into this subject. At present the drag and side force formulations developed by the author do not account for any other "appendages" than keel, skeg

and rudder.

B. MORLEY: Your estimations of trends in performance of 12 Metre Yachts assume calm water. How valid are the results for a wind speed in excess of about 14 knots in which case the sea conditions can be described as quite rough.

P. VAN OOSSANEN: No account is given in the paper concerning the effect of waves. Calculations of the added resistance in waves have shown, however, that generally added resistance increases with displacement. The main conclusion of the author's study on the optimum size of 12 Metre Class Yachts for the America's Cup would, on this basis, not be incorrect. There are a number of additional factors to be considered when dealing with the performance in waves, however, which have not yet been addressed.

Additional references:

(1) J. Gerritsma, G. Moeijes and R. Onnink: "Test Results of a Systematic Yacht Hull Series" 5th HISWA Symposium on Developments of Interest to Yacht Architecture, HISWA, Amsterdam, 1977.

(2) J. Gerritsma, R. Onnink and A. Versluis; "Geometry, Resistance and stability of the Delft Systemactic Yacht Hull Series" 7th HISWA Symposium on Developments of Interest to Yacht Architecture, HISWA, Amsterdam, 1981.

(3) G.S. Hazen " A Model of Sail Aerodynamics for Diverse Rig Types", SNAME, New England Sailing Yacht Symposium, New London, Connecticut, March 22, 1980.